THE MAXIMAL NUMBER OF EXCEPTIONAL DEHN SURGERIES

MARC LACKENBY AND ROBERT MEYERHOFF

1. Introduction

Thurston's hyperbolic Dehn surgery theorem is one of the most important results in 3-manifold theory, and it has stimulated an enormous amount of research. If M is a compact orientable hyperbolic 3-manifold with boundary a single torus, then the theorem asserts that, for all but finitely many slopes s on ∂M, the manifold $M(s)$ obtained by Dehn filling along s also admits a hyperbolic structure. The slopes s where $M(s)$ is not hyperbolic are known as *exceptional*. A major open question has been: what is the maximal number of exceptional slopes on such a manifold M? When M is the exterior of the figure-eight knot, the number of exceptional slopes is 10, and this was conjectured by Gordon in [20] to be an upper bound that holds for all M. In this paper, we prove this conjecture.

Theorem 1.1. *Let M be a compact orientable 3-manifold with boundary a torus, and with interior admitting a complete finite-volume hyperbolic structure. Then the number of exceptional slopes on ∂M is at most* 10.

Although it is not our approach, much of the progress on this problem has been achieved by bounding the intersection number $\Delta(s_1, s_2)$ between exceptional slopes s_1 and s_2. It was conjectured by Gordon [20] that $\Delta(s_1, s_2)$ is always at most 8, a bound which is attained for the exteriors of the figure-eight knot and the figure-eight knot sister. A huge amount of effort has been made on this conjecture, with some notable progress in [2, 3, 4, 6, 7, 8, 11, 21, 22, 23, 26]; see [5] for a survey. We also prove this conjecture.

Theorem 1.2. *Let M be a compact orientable 3-manifold with boundary a torus, and with interior admitting a complete finite-volume hyperbolic structure. If s_1 and s_2 are exceptional slopes on ∂M, then their intersection number $\Delta(s_1, s_2)$ is at most* 8.

Recently and using different methods, Agol [3] has shown that, for all but finitely many 3-manifolds M as in Theorem 1.1, the intersection number between exceptional slopes is at most 5 and the number of exceptional slopes is at most 8. Moreover, there is an algorithm to compute the list of excluded manifolds. However, the algorithm is far from practical, and so there seems, at present, to be no way of using Agol's theorem to prove Gordon's conjectures.

Theorems 1.1 and 1.2 are proved using a combination of new geometric techniques and a rigorous computer-assisted calculation. In particular, an improved

First author supported by an EPSRC Advanced Research Fellowship.
Second author partially supported by NSF grants DMS-0553787 and DMS-0204311.

version of the 6-theorem of Lackenby [26] and Agol [2] is established, and extensive use of the Mom technology of Gabai, Meyerhoff and Milley ([16], [17]) is required.

In Mom theory, the following list of 2-cusped and 3-cusped hyperbolic 3-manifolds plays a central role, where the notation is that of the census [10] of hyperbolic 3-manifolds:

$m412$	$s596$	$s647$	$s774$	$s776$	$s780$	$s785$	$s898$	$s959$

FIGURE 1

The proof of Theorems 1.1 and 1.2 immediately divides into two cases: either M is obtained by Dehn filling one of the manifolds in this list, or it is not. In the former case, a straightforward analysis using the computer program Snap [19] leads to a proof of the theorems (see Section 8). The other case is when M is not obtained by Dehn filling one of the manifolds in this list. We consider the inverse image in $\mathbb{H}^3$ of a maximal horoball neighborhood of the cusp of M, which is a collection of horoballs. Following [16] and [17], we extract three real-valued parameters from this arrangement, which are denoted e_2, e_3 and e_4. (More details can be found in Section 3.) We also define three other real-valued parameters, m, t and h, which encode the shape and size of the cusp torus. These 6 parameters then define a parameter space. We show that outside an explicit compact region of this parameter space, the theorems hold. We then examine this compact region using a rigorous computer analysis. We divide the region into small pieces, and show that, in each piece, the theorems hold. This requires two approaches. We develop new geometric tools which can be used to deduce that, in certain regions, either a contradiction is reached or M contains a 'torus-friendly geometric Mom-2 or Mom-3' and hence is obtained by Dehn filling one of the manifolds in Figure 1. If we cannot exclude a region, then we need to bound the number of exceptional slopes in the boundary torus and their intersection numbers. Prior to the present paper, this amounted to using the 6-theorem and checking whether or not the length of the slope was at most 6. However, for our purposes, this is not strong enough and so we prove an enhanced version of the 6-theorem, which depends on the parameter e_2.

The plan of the paper is as follows. In Section 2, we give a historical survey of the problem. In Section 3, we recall the terminology and techniques of Mom structures. In Section 4, we prove the extension of the 6-theorem. In Section 5, we derive lower bounds on the area of the cusp torus. In Section 6, we give the geometric arguments that underpin the parameter space analysis. In Section 7, we give details of the rigorous computation. In Section 8, we examine the manifolds that are obtained by Dehn filling one of the manifolds from Figure 1, and prove the theorems in this case.

ACKNOWLEDGEMENTS. We thank the Institute for Advanced Study, Princeton. The second-named author was a member at the Institute during the beginning of this research, and the first-named author was visiting the Institute when our collaboration began. We also thank the referees of this paper for their thorough and careful reading of it, and for their helpful suggestions which have substantially improved it.

2. Historical survey

There have been at least four parallel approaches to the Dehn surgery problem. The most popular method, with the most extensive literature, has been topological. Here, one seeks not to establish that the filled-in manifold $M(s)$ has a hyperbolic structure, but rather that it is 'hyperbolike'. The precise definition of this term varies according to the context, but the gist is that a compact orientable 3-manifold is hyperbolike if it has topological properties that are equivalent to the existence of a hyperbolic structure, assuming the geometrisation conjecture. Thus, now that Perelman's proof of this conjecture ([34], [35], [36]) is accepted as correct ([30], [31], [25]), a compact orientable 3-manifold is hyperbolike if and only if it is hyperbolic. In the topological approach, $M(s)$ is hyperbolike if it is irreducible, atoroidal and not a Seifert fibre space. One considers slopes s_1 and s_2 where neither $M(s_1)$ nor $M(s_2)$ is hyperbolike and one seeks to bound their intersection number $\Delta(s_1, s_2)$. For example, if $M(s_1)$ and $M(s_2)$ are both reducible, then they contain essential 2-spheres, which restrict to essential planar surfaces in M. One considers the intersection pattern of these surfaces and, after some subtle and beautiful combinatorics, very accurate bounds on $\Delta(s_1, s_2)$ can be achieved. In fact, in this case, Gordon and Luecke [21] proved that $\Delta(s_1, s_2) \leq 1$, and so there are at most 3 slopes s on M for which $M(s)$ is reducible. In addition, the $\mathrm{SL}(2, \mathbb{C})$ representation variety has been used extensively in this approach. Many mathematicians have been part of this program, including Boyer, Culler, Gordon, Luecke, Scharlemann, Shalen, Wu and Zhang (see [5] for a survey). However, the case where $M(s_1)$ or $M(s_2)$ is an atoroidal Seifert fibre space has proved to be problematic. When it has finite fundamental group, the methods of Boyer and Zhang [8] have been very successful, but when it does not, the situation is harder to handle topologically, and little progress has been made.

A second approach has been via foliations and laminations. Here, the aim is to find an essential foliation or lamination on $M(s)$. By Novikov's theorem [33], this implies that $M(s)$ is irreducible or $S^2 \times S^1$ (and one can typically rule out the latter case). Moreover, if the essential lamination is genuine, then $M(s)$ is hyperbolike, by Gabai and Kazez's theorem [14]. According to a result of Gabai [32], there is a slope λ such that $M(s)$ has a genuine essential lamination provided $\Delta(s, \lambda) \geq 3$. But unfortunately, the number of excluded slopes, where $\Delta(s, \lambda) \leq 2$, is not finite. Nevertheless, the foliation and lamination approach has been extremely successful, notably with Gabai's proof [12] of the Property R conjecture.

A third approach, due to Hodgson and Kerckhoff [23], aims to prove that $M(s)$ is hyperbolic without appealing to the geometrisation conjecture. Since their methods predate Perelman's work, this was the first approach to yield a universal upper bound (60) on the number of exceptional slopes, independent of the manifold M.

The fourth approach has also been geometric, but with the aim of deducing a weaker conclusion on $M(s)$ than hyperbolicity. The first result in this direction was the Gromov-Thurston 2π-theorem [4] which established a universal upper bound on the number of slopes s for which $M(s)$ does not admit a Riemannian metric of negative curvature. This upper bound, due to Thurston, was 48. However, there were successive improvements to this bound. Bleiler and Hodgson reduced it to 24 in [4]. By applying work of Cao and Meyerhoff [9], this could be reduced to 14.

A continuation of this approach was the 6-theorem of Lackenby [26] and Agol [2], which reduced the number of excluded slopes to 12. However, outside this set

of excluded slopes, $M(s)$ is shown only to be irreducible, atoroidal, and not Seifert fibered, and to have infinite, word-hyperbolic fundamental group. But with the solution of the geometrisation conjecture by Perelman, any compact orientable 3-manifold satisfying these conditions must also admit a hyperbolic structure. Thus, as a consequence of Perelman's work, the number of exceptional slopes on M is established by this approach to be at most 12.

The 2π-theorem and 6-theorem both are phrased in terms of the length of a slope s. Here, one considers the unique maximal horoball neighbourhood of the cusp of M, and its immersed boundary torus, which we term the *cusp torus*. One defines the *length* of s to be the length of shortest curve on this torus with slope s. If the length of s is more than 2π, then $M(s)$ admits a negatively curved Riemannian metric. If the length is more than 6, then $M(s)$ is irreducible, atoroidal, and not Seifert fibered, and has infinite, word-hyperbolic fundamental group. Thurston gave an upper bound of 48 on the number of slopes with length at most 2π.

The argument that leads to the bound of 48 is instructive. Using elementary means, Thurston showed that the length of each slope is at least 1. Thus, it is clear that, for any fixed constant L, there is a uniform upper bound on the number of slopes with length at most L. To actually find this upper bound, one can argue as follows. The universal cover of the cusp torus is a Euclidean plane, and the inverse image of a basepoint is a lattice in this plane. The fact that each slope has length at least 1 forces every pair of lattice points to be at least distance 1 apart. Thus, the minimal possible co-area of such a lattice is $\sqrt{3}/2$, which is achieved by the hexagonal lattice, by Thue's theorem. The area A of the cusp torus is therefore at least $\sqrt{3}/2$. An elementary argument (see the proof of Theorem 8.1 in [2] for example) gives that the intersection number of two slopes with length ℓ_1 and ℓ_2 is at most $\ell_1\ell_2/A$. When $\ell_1, \ell_2 \leq 2\pi$ and $A \geq \sqrt{3}/2$, the intersection number is therefore at most 45. Lemma 8.2 in [2] states that, if E is any collection of slopes on a torus, where any two slopes in E have intersection number at most Δ, then $|E| \leq p+1$, where p is any prime more than Δ. (Note that this bound is not always sharp. For example, if $\Delta = 7$, then $|E|$ can be shown to be at most 10.) Setting $p = 47$ gives the upper bound.

Thus, the quantity $\ell_1\ell_2/A$ is central to the fourth approach to the Dehn surgery problem. Increasingly good upper bounds on $\ell_1\ell_2/A$, when ℓ_1 and ℓ_2 are the lengths of exceptional slopes, have been found. The 6-theorem reduced the critical value of ℓ_1 and ℓ_2 from 2π to 6. But, the most significant progress has been achieved by finding improved lower bounds on A, the area of the cusp torus. Adams [1] increased the lower bound on A to $\sqrt{3}$, which gave the upper bound of 24 exceptional slopes. Then Cao and Meyerhoff [9] gave a lower bound of 3.35 for A, which led to the upper bound of 12 exceptional slopes. Recently, the work of Gabai, Meyerhoff and Milley ([16], [17]) improves the lower bound for A to 3.7, provided that M is not obtained by Dehn filling one of the manifolds in Figure 1. This result is not explicitly stated in their paper, but it follows from their methods. This leads to an upper bound of 9 on the intersection number of any two exceptional slopes, but unfortunately, it does not decrease the bound on the number of exceptional slopes below 12. In fact, the following table, taken from [5], gives the maximal size of a set of slopes, such that any two slopes in this set have intersection number at most Δ.

Maximal intersection number Δ	0	1	2	3	4	5	6	7	8	9	10
Maximal number of slopes	1	3	4	6	6	8	8	10	12	12	12

So, reducing the upper bound on the number of exceptional slopes from 12 to 10 is not as straightforward as it first appears. If one were to prove the bound of 10 using intersection numbers, then one would have to improve the known bounds on intersections numbers from 9 to 7, which is quite a significant reduction.

In addition, there is an example of Agol that illustrates some difficulties. If one wants to develop the fourth approach to the problem, it seems that either one must improve the 6-theorem yet further, by reducing the critical slope length below 6, or one must show that M always has at most 10 slopes with length at most 6. But neither of these steps is possible. Agol [2] examined the case where M is the exterior of the figure-eight knot sister. This has two key properties: it has 12 slopes with length at most 6, *and* it has exceptional slopes with length precisely 6. Fortunately, this manifold is obtained by Dehn filling $s776$, which appears in Figure 1. Thus, by work of Gabai, Milley and Meyerhoff ([16], [17]) it falls into a family of well-understood exceptions. In fact, it is by melding the Mom technology with some new geometric results, specifically tailored to the Dehn surgery problem, that we are able to prove Theorems 1.1 and 1.2.

3. Mom terminology and results

The Mom technology of Gabai, Meyerhoff and Milley [16] plays a key role in this paper. In this section, we recall the Mom terminology and results.

Let M be a compact orientable 3-manifold with boundary a torus, and with interior admitting a complete finite-volume hyperbolic structure. The universal cover of $M - \partial M$ is hyperbolic 3-space $\mathbb{H}^3$, for which we use the upper half-space model. The inverse image in $\mathbb{H}^3$ of a maximal horoball neighbourhood of the cusp is a union of horoballs $\{B_i\}$. We may arrange that one of these horoballs, denoted B_∞, is $\{(x, y, z) : z \geq 1\}$. Given two horoballs B_i and B_j, neither equal to B_∞, we say that B_i and B_j are in the same *orthoclass* (with respect to B_∞) if either B_i and B_j differ by a covering transformation that preserves B_∞ or there exists some covering transformation g such that $g(B_i) = B_\infty$ and $g(B_\infty) = B_j$. We denote the orthoclasses by $\mathcal{O}(1)$, $\mathcal{O}(2)$, and so forth. For any $B \in \mathcal{O}(n)$, we call $d(B, B_\infty)$ the *orthodistance* of B and denote it $o(n)$. We order the orthoclasses in such a way that the corresponding orthodistances are non-decreasing. Since the horoball neighbourhood of the cusps is maximal, there is one B_i that touches B_∞, and hence $o(1) = 0$. It is convenient also to define the quantity $e_n = \exp(o(n)/2)$. Thus e_n is a non-decreasing sequence starting at $e_1 = 1$. In the upper half-space model, the Euclidean diameter of $B \in \mathcal{O}(n)$ is e_n^{-2}. The *orthocenter* of a horoball B_i other than B_∞ is the closest point on B_∞ to B_i. We say that two horoballs B_i and B_j are in the $\mathcal{O}(n)$ *orthopair class* if there is a covering transformation g such that $g(B_i) = B_\infty$ and $g(B_j) \in \mathcal{O}(n)$. We then say that B_i and B_j are $o(n)$*-separated*.

A (p, q, r)*-triple* is a triple of horoballs $\{B_1, B_2, B_3\}$ such that B_1, B_2 are in the $\mathcal{O}(r)$ orthopair class, B_2, B_3 are in the $\mathcal{O}(p)$ orthopair class and B_1, B_3 are in the $\mathcal{O}(q)$ orthopair class, possibly after re-ordering. A *geometric Mom-n structure* is a collection of n triples of type $(p_1, q_1, r_1), \ldots, (p_n, q_n, r_n)$, no two of which are equivalent under the action of $\pi_1(M)$, and such that the indices p_i, q_i and r_i all come from the same n-element subset of $\mathbb{Z}_+$. We say that the Mom-n structure

involves $\mathcal{O}(k)$ if $k \in \{p_1, q_1, r_1, \ldots, p_n, q_n, r_n\}$. A geometric Mom-$n$ is *torus-friendly* if $n = 2$ or if $n = 3$ and the Mom-3 does not possess exactly two triples of type (p, q, r) for any set of distinct positive indices p, q and r.

The first key lemma, which appears as Corollary 3.3 in [17], is as follows.

Lemma 3.1. *For any integer n, there are no (n, n, n)-triples.*

In particular, there are no $(1, 1, 1)$-triples. Hence, the Euclidean distance in ∂B_∞ between the orthocenters of two $\mathcal{O}(1)$-horoballs is at least e_2. More generally, one can compute the distance between orthocenters using the following elementary lemma (Lemma 3.4 in [17]).

Lemma 3.2. *Suppose that $B_1 \in \mathcal{O}(q)$, $B_2 \in \mathcal{O}(r)$, and that B_1 and B_2 are $o(p)$-separated. Then the Euclidean distance between the orthocenters of B_1 and B_2 is $e_p/(e_q e_r)$.*

The following results will be crucial. These are contained in [17] but not explicitly stated there. We include here only a brief outline of their proof.

Theorem 3.3. *If M contains a geometric Mom-2 involving $\mathcal{O}(1)$ and $\mathcal{O}(n)$, then either $e_n \geq 1.5152$ or M is obtained by Dehn filling one of the manifolds $m125$, $m129$ or $m203$.*

Note that the manifolds $m125$, $m129$ or $m203$ are obtained by Dehn filling $s776$, which appears in Figure 1.

Theorem 3.4. *If M contains a torus-friendly geometric Mom-3 involving $\mathcal{O}(1)$, $\mathcal{O}(2)$ and $\mathcal{O}(3)$, then either $e_3 \geq 1.5152$ or M is obtained by Dehn filling one of the manifolds in Figure 1.*

Proof of Theorems 3.3 and 3.4: Suppose first that M contains a geometric Mom-2 involving $\mathcal{O}(1)$ and $\mathcal{O}(n)$. Associated to this, there is a cell complex Δ, defined in [17]. If $e_n < 1.5152$, the material in Section 6 of [17] gives that Δ is embedded. Then Theorem 7.1 and Proposition 8.2 of [17] give that M is obtained by Dehn filling a 'full topological internal Mom-2 structure'. By Theorem 5.1 of [16], there are only 3 hyperbolic manifolds with such a structure: $m125$, $m129$ and $m203$.

Suppose now that M contains a torus-friendly geometric Mom-3 involving $\mathcal{O}(1)$, $\mathcal{O}(2)$ and $\mathcal{O}(3)$ but not a geometric Mom-2 involving a subset of $\mathcal{O}(1)$, $\mathcal{O}(2)$ and $\mathcal{O}(3)$. Then, if $e_3 < 1.5152$, the associated cell complex is embedded. Theorems 7.1 and 8.3 of [17] give that M is obtained by Dehn filling a 'full topological internal Mom-3 structure'. By Theorem 5.1 of [16], any hyperbolic manifold admitting such a structure is obtained by Dehn filling one of the manifolds in Figure 1. □

4. An improvement to the 6-theorem

In this section, we prove the following result, which is a version of the 6-theorem that depends on the parameter e_2.

Theorem 4.1. *Let M be a compact orientable 3-manifold, with boundary a torus and with interior admitting a complete finite-volume hyperbolic structure. Let s be a slope on ∂M with length at least*

$$\frac{\pi e_2}{\arcsin(e_2/2)}$$

if $e_2 \leq \sqrt{2}$*, and length at least*

$$\frac{2\pi e_2}{2\arcsin(\sqrt{1-e_2^{-2}}) + e_2^2 - 2\sqrt{e_2^2-1}}$$

if $e_2 > \sqrt{2}$*. Then,* $M(s)$ *is hyperbolic.*

We denote by $L(e_2)$ the critical slope length that is given in the above result. A graph of $L(e_2)$ is shown in Figure 2. When $e_2 = 1$, Theorem 4.1 gives the same critical slope length as the 6-theorem. But as e_2 increases, the critical slope length decreases, tending to zero.

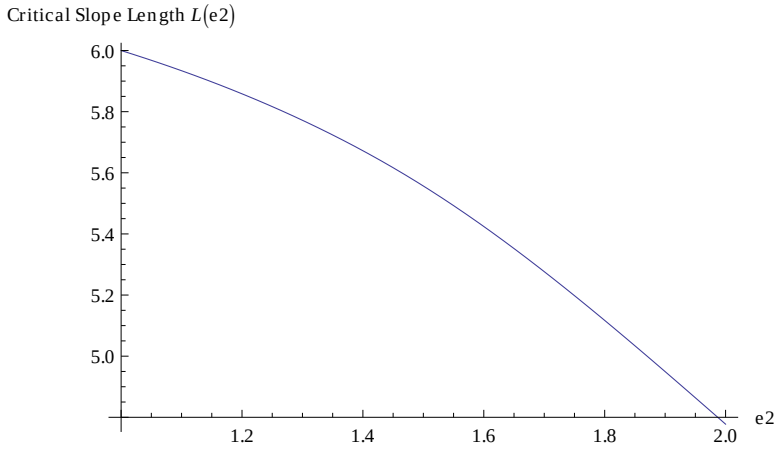

FIGURE 2

We start by recalling an outline of the proof of the 6-theorem. The proof of Theorem 4.1 will be a refinement of this. Suppose that $M(s)$ is not hyperbolic. We wish to show that the length of s is at most 6. Suppose, for simplicity, that $M(s)$ contains an essential sphere. By choosing this sphere suitably, we may arrange that its intersection F with M is incompressible and boundary-incompressible and that each boundary component of F has slope s. We may then homotope F to a pleated surface. Its area is then at most $-2\pi\chi(F) = 2\pi(|\partial F| - 2)$. The aim is to show geometrically that each component of ∂F contributes at least $(\pi/3)$ times the length of s to the area of F. Thus, if the length of each s is more than 6, then the area of F is at least $(\pi/3)6|\partial F| = 2\pi|\partial F|$, which is a contradiction. The intersection of F with the maximal horoball neighbourhood of the cusps is a collection of copies of $S^1 \times [1, \infty)$ plus possibly some compact components. Each copy of $S^1 \times [1, \infty)$ is ambient isotopic to a vertical surface lying over a curve of slope s in the cusp torus. Its area is therefore at least the length of s. Thus, each component of ∂F contributes at least Length(s) to the area of F. However, we want to improve this contribution to $(\pi/3)$Length(s), and to do this, one must consider the parts of F not lying in the horoball neighbourhood of the cusps. The most convenient way to do this is to consider the associated geodesic spine S, which is defined as follows.

The inverse image in $\mathbb{H}^3$ of the maximal horoball neighbourhood of the cusp is a collection $\{B_i\}$ of horoballs. One of these, B_∞, has been fixed as $\{(x, y, z) : z \geq 1\}$ in the upper half-space model. Let $\tilde{S}$ be the set of points in $\mathbb{H}^3$ that do not

have a unique closest point in $\bigcup B_i$. It is invariant under the group of covering transformations, and its quotient in M is S. This is a spine for M, in which each cell is totally geodesic. Thus, $M - S$ is a neighbourhood of the cusp that is larger than the interior of the maximal horoball neighbourhood. By considering the area of F in $M - S$, we obtain the improved area contribution of $(\pi/3)\text{Length}(s)$. Specifically, the following result is used, which appears as Lemma 3.3 in [26].

Lemma 4.2. *Let M be a compact orientable 3-manifold, with boundary a torus and with interior admitting a complete finite-volume hyperbolic structure. Let S be a geodesic spine arising from a horoball neighbourhood of the cusp of $M - \partial M$. Let G be a compact orientable (possibly non-embedded) surface with interior in $M - S$, with boundary in $\partial M \cup S$ and with $\partial G \cap \partial M$ representing $\pm k[s] \in H_1(\partial M)$, where $k \in \mathbb{N}$ and s is some slope. Then*

$$\text{Area}(G - \partial M) \geq k\,(\pi/3)\text{Length}(s).$$

By applying this to each component of the surface $F - S$, we obtain the 6-theorem, at least when $M(s)$ is reducible.

If $M(s)$ has finite fundamental group, then the core of the surgery solid torus has finite order. So, some power of this core curve bounds a disk in $M(s)$. The restriction of this disk to M is a compact planar surface F, with all but one boundary component having slope s. We apply the above argument to this surface.

To show that $\pi_1(M(s))$ is word hyperbolic, we use Gabai's ubiquity theorem [13], as stated as Theorem 2.1 in [26]. We consider an arbitrary loop K in M that is homotopically trivial in $M(s)$. There is therefore a compact planar surface F, with one boundary component mapped to K, and the remaining boundary components mapped to non-zero multiples of the slope s. We may assume that F is homotopically incompressible and homotopically boundary-incompressible (as defined in [26]). The aim is to show that $|F \cap \partial M|$ is bounded above by $c\,\text{Length}(K)$, where c is a constant depending on M and s, but not K. Theorem 2.1 in [26] then implies that $\pi_1(M(s))$ is word hyperbolic. In order to establish this bound, we again consider the area of F, but the argument is slightly more complicated. The detailed proof appears in [26].

Finally, if $M(s)$ is irreducible, and has infinite, word hyperbolic fundamental group, then it is atoroidal and not Seifert fibred. Thus, the 6-theorem is established.

Let us now define a function $I(e_2)$, which will turn out to be the improvement factor in the critical slope length, as compared with the 2π theorem. When $e_2 \leq \sqrt{2}$,

$$I(e_2) = \frac{2\arcsin(e_2/2)}{e_2}.$$

When $e_2 > \sqrt{2}$,

$$I(e_2) = \frac{2\arcsin(\sqrt{1-(1/e_2^2)}) + e_2^2 - 2\sqrt{e_2^2 - 1}}{e_2}.$$

In order to prove Theorem 4.1, we need the following proposition, which is an improvement on Lemma 4.2.

Proposition 4.3. *Let M, S, G and k be as in Lemma 4.2. Then the area of $G - \partial M$ is at least $k\,\text{Length}(s)I(e_2)$.*

Thus, the critical slope length is improved to $2\pi/I(e_2)$, thereby proving Theorem 4.1.

We now briefly explain the proof of Lemma 4.2, as its main ideas will be used in the proof of Proposition 4.3. We start by introducing some terminology. Let M, S, G and k be as in Lemma 4.2. Recall that $\tilde{S}$ is the inverse image of S in $\mathbb{H}^3$. Let $\tilde{E}$ be the closure of the component of $\mathbb{H}^3 - \tilde{S}$ that contains B_∞. For each horoball B_i of $\{B_i\}$ other than B_∞, let P_i be the totally geodesic plane equidistant between B_∞ and B_i. Let h be a positive real number. Let $\tilde{Q}_h$ be the set of points in $\{z = h\}$ that lie above $\tilde{S}$. (See Figure 3.) Let Q_h be the quotient of $\tilde{Q}_h$ by the stabiliser of B_∞. Then Q_h is an embedded surface in $M - S$, and $\bigcup_{h\in(0,\infty)} Q_h = M - S$. Let $\tilde{E}_h$ be the set of points in $\mathbb{H}^3$ that lie above $\tilde{S} \cup \{z = h\}$, and let E_h be the quotient of $\tilde{E}_h$ by the stabiliser of B_∞. Thus, E_h is the set of points in $M - S$ between Q_h and the cusp. (See Figure 4.)

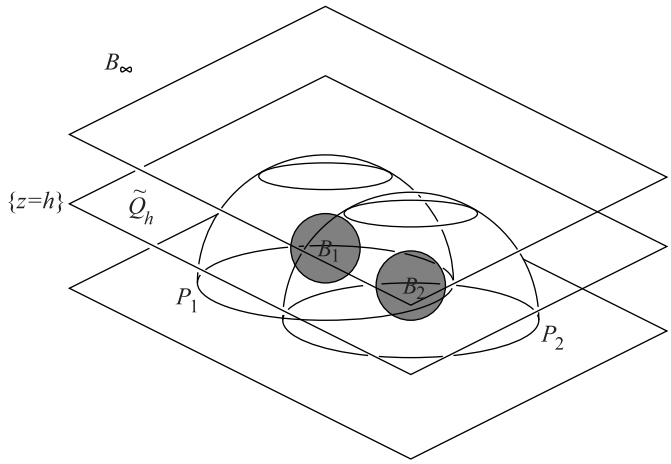

FIGURE 3

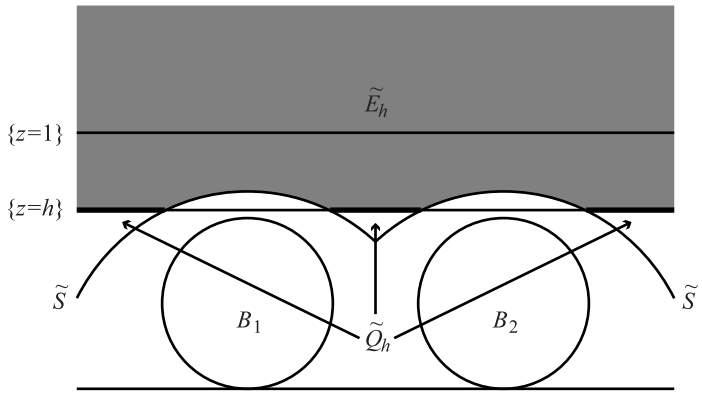

FIGURE 4

We may assume, by performing an arbitrarily small perturbation of the surface G, that, for all but finitely many values of h, $G \cap Q_h$ is a finite collection of immersed arcs. The area of G is at least

$$\int_0^\infty \frac{\text{Length}(G \cap Q_h)}{h}\, dh.$$

The proof of Lemma 4.2 proceeded by examining $\text{Length}(G \cap Q_h)/(k\ \text{Length}(s))$. It was shown that this ratio is minimised by a certain surface in the figure-eight knot complement. In this case, the orthocenters of the $\mathcal{O}(1)$ and $\mathcal{O}(2)$ horoballs form a hexagonal lattice. Taking a vertical slice through these, we see an arrangement of horoballs and spine as in Figure 5. In the proof of Lemma 4.2, it was shown that the ratio $\text{Length}(G \cap Q_h)/(k\ \text{Length}(s))$ is minimised by the intersection of $\{z = h\}$ with the shaded surface. Hence, integrating with respect to h, we get that $\text{Area}(G)/(k\ \text{Length}(s))$ is at least that of the shaded surface. But this surface has area $\pi/3$ and contributes 1 to slope length. This is why the ratio $\pi/3$ appears in Lemma 4.2.

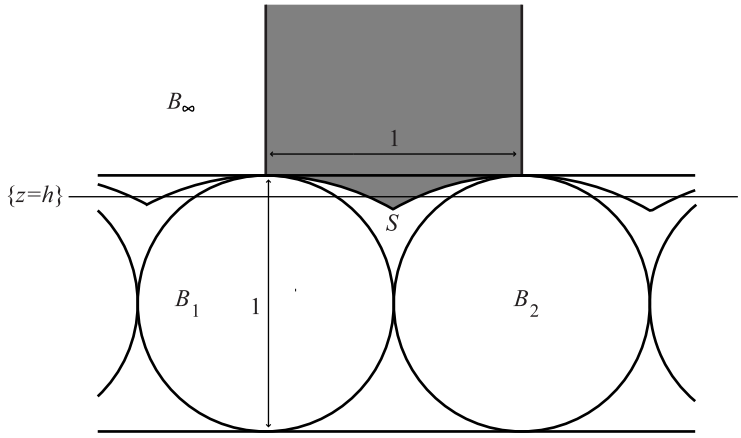

FIGURE 5

We now explain the proof of Proposition 4.3. When e_2 is bigger than 1, the $\mathcal{O}(1)$ horoballs cannot be tangent. In fact, their orthocenters are at least e_2 apart in the Euclidean metric on ∂B_∞. Hence, one should be considering an arrangement as in Figure 6. The area of the shaded region is $2\arcsin(e_2/2)$ and its contribution to slope length is e_2. The ratio of these quantities is $I(e_2)$, when $e_2 \leq \sqrt{2}$.

When $e_2 > \sqrt{2}$, we again must consider two $\mathcal{O}(1)$ horoballs, but due to the intervention of other smaller horoballs, it turns out that we must restrict attention to points above $\{z = 1/e_2\}$. Thus, we must consider a configuration as in Figure 7. Here, the shaded region has area

$$2\arcsin(\sqrt{1 - (1/e_2^2)}) + e_2^2 - 2\sqrt{e_2^2 - 1}$$

and it contributes e_2 to slope length. Thus, again, the ratio of these quantities is $I(e_2)$. To prove Proposition 4.3, we must show why these two horoball arrangements are the critical configurations.

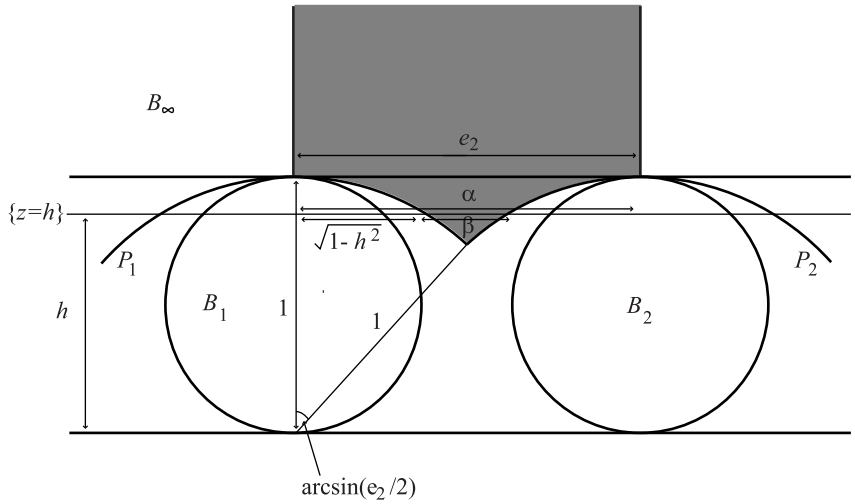

FIGURE 6

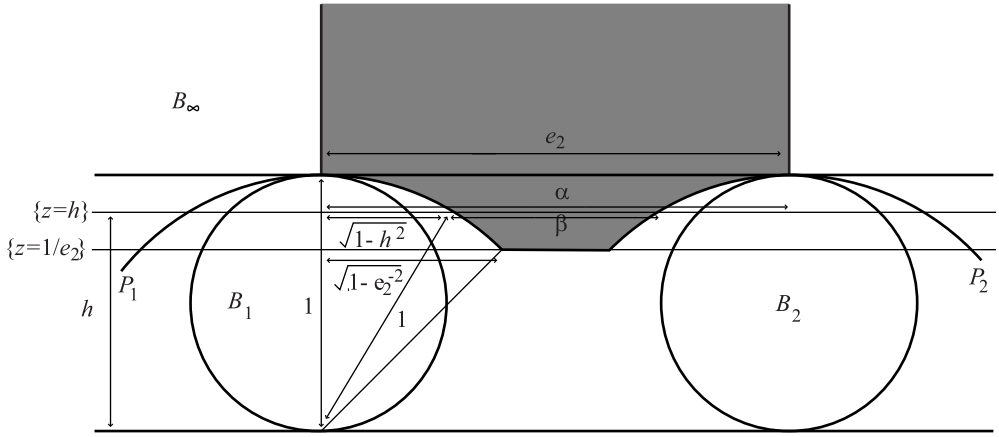

FIGURE 7

Proof of Proposition 4.3. As above, we may assume that, for all but finitely many values of h, $G \cap Q_h$ is a finite collection of immersed arcs. The area of G is at least

$$\int_0^\infty \frac{\text{Length}(G \cap Q_h)}{h}\, dh.$$

Since the aim of the proposition is to find a lower bound on the area of G, we therefore will bound the length of $G \cap Q_h$ from below by a function of h. Let us first consider the case when $h > 1$. Then $Q_h = \partial E_h$ is a torus. The surface $G \cap E_h$ forms a homology between $G \cap Q_h$ and $\pm k[s]$ in ∂M. But any collection of curves in Q_h homologous to $\pm k[s]$ must have length at least $k\,\text{Length}(s)/h$.

Let us now focus on the case where $0 < h \leq 1$. We define a function

$$\mathrm{RelLength}(e_2, h) = \begin{cases} 1 & \text{if } h \geq 1; \\ \max\left\{0, 1 - \frac{2}{e_2}\sqrt{1-h^2}\right\} & \text{if } \min\{1/\sqrt{2}, 1/e_2\} \leq h \leq 1; \\ 0 & \text{otherwise.} \end{cases}$$

Geometrically, this is the ratio of the lengths of β to α in Figure 6 (if $e_2 \leq \sqrt{2}$) and Figure 7 (if $e_2 > \sqrt{2}$). Hence,

$$\int_0^\infty \frac{e_2 \,\mathrm{RelLength}(e_2, h)}{h^2} dh$$

is the area of the shaded region in Figure 6 or Figure 7, which is $I(e_2)e_2$.

Claim 1. The length of $G \cap Q_h$ is at least

$$k \,\mathrm{Length}(s) \frac{\mathrm{RelLength}(e_2, h)}{h}.$$

Thus, the claim asserts that, when $e_2 \leq \sqrt{2}$, the critical configuration is shown in Figure 6, whereas when $e_2 > \sqrt{2}$, the critical configuration is shown in Figure 7.

Let us assume the claim for a moment. Then, the area of G is at least

$$\begin{aligned} \int_0^\infty \frac{\mathrm{Length}(G \cap Q_h)}{h}\, dh &\geq \frac{k \,\mathrm{Length}(s)}{e_2} \int_0^\infty \frac{e_2 \,\mathrm{RelLength}(e_2, h)}{h^2} dh \\ &= k \,\mathrm{Length}(s) I(e_2), \end{aligned}$$

thereby proving Proposition 4.3.

It is convenient to give ∂E_h the metric pulled back via the vertical projection $\partial E_h \to \{z = h\}$. It then becomes a Euclidean torus.

The arcs $G \cap Q_h$ extend to a collection of closed curves $G \cap \partial E_h$. The surface $G \cap E_h$ forms a homology between $G \cap \partial E_h$ and $\pm k[s]$ in ∂M. Hence, the length of $G \cap \partial E_h$ is at least $k \,\mathrm{Length}(s)/h$. We wish to bound from below the length of the parts of $G \cap \partial E_h$ that lie in Q_h.

We will shortly homotope $G \cap \partial E_h$ in ∂E_h, creating new curves C_h. We will ensure that the length of $C_h \cap Q_h$ is at most that of $G \cap Q_h$. Thus, if we can show that $C_h \cap Q_h$ satisfies the required lower bound on length, the claim will be proved.

So, consider an arc of $G \cap Q_h$. We will now extend it to a curve which sits in the Euclidean torus ∂E_h. The endpoints of the arc lie on totally geodesic faces of S, called P_1 and P_2, say. We now consider two possibilities.

(1) If this arc is not homotopic into S, then replace it by the geodesic arc that runs between the points on P_1 and P_2 that are closest to ∂B_∞.
(2) On the other hand, if the arc is homotopic into S, perform this homotopy, replacing it by a concatenation of Euclidean geodesic arcs in S, each of which runs between the highest points of two incident faces of S.

In case (1), the resulting geodesic arc may intersect faces of S that the old arc did not. If so, repeat this procedure. (See Figure 8.) It is clear that, at each stage of the procedure, the length of $G \cap Q_h$ decreases. We now show that the procedure is guaranteed to terminate.

After the first stage of the procedure, $G \cap \partial E_h$ is a concatenation of geodesic arcs in ∂E_h, each of which joins the highest points of two faces of S. Define the *reduced length* of such an arc to be the length in ∂E_h of the parts of the arc that remain when

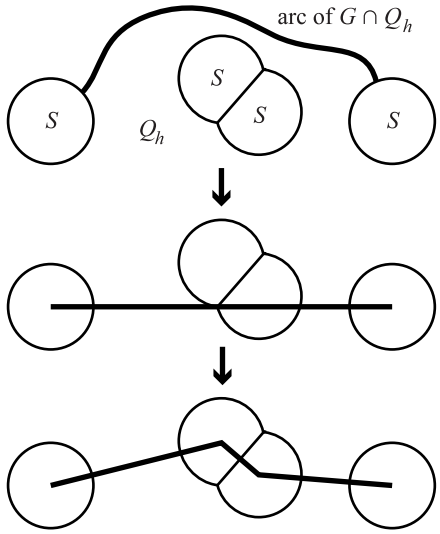

FIGURE 8. Straightening the arcs $G \cap Q_h$

its intersection between the initial and terminal faces of S are removed. Define the *reduced length* of $G \cap \partial E_h$ to be the sum of the reduced lengths of its arcs. Then, the reduced length of each arc in $G \cap \partial E_h$ is, after the first stage of the procedure, at most some constant C, say. Now, there are only finitely many geodesic arcs in ∂E_h which join the highest points on faces of S and which have reduced length in the interval $(0, C]$. Consider all such arcs, and let $0 < \ell_1 \leq \ell_2 \leq \cdots \leq \ell_n$ be their reduced lengths. Then, let ϵ be the smallest positive value of $\ell_i - \sum_{i=1}^{n} c_j \ell_j$, where $1 \leq i \leq n$ and each c_j is a non-negative integer. Then, at each stage of the procedure, the reduced length of $G \cap \partial E_h$ decreases by at least ϵ, since at least one arc joining the highest points of two faces of S is removed and replaced by arcs with smaller total reduced length. Thus, this procedure does indeed terminate.

The resulting curves C_h are a concatenation of arcs, each of which is a geodesic in ∂E_h running between the highest points of two faces of S. Moreover, each such arc α either lies entirely in S or intersects only the faces of S that contain its endpoints. Thus, the intersection of α with S is either all of α or two sub-intervals of α, each of which contains an endpoint of α. Since the curves C_h are homologous to $\pm k[s]$, we obtain the inequality

$$\sum_{\alpha} \text{Length}(\alpha) = \text{Length}(C_h) \geq \frac{k \, \text{Length}(s)}{h}.$$

We now define a new function:

$$\text{RelLength}_2(e_2, h) = \max\left\{0, 1 - e_2\sqrt{1-h^2} - \sqrt{\max\{0, 1 - e_2^2 h^2\}}\right\}.$$

Geometrically, this is the ratio of the lengths of β to α in Figure 9.

Claim 2. When $e_2 \leq \sqrt{2}$,

$$\frac{\text{Length}(\alpha \cap Q_h)}{\text{Length}(\alpha)} \geq \min\{\text{RelLength}(e_2, h), \text{RelLength}_2(e_2, h)\}.$$

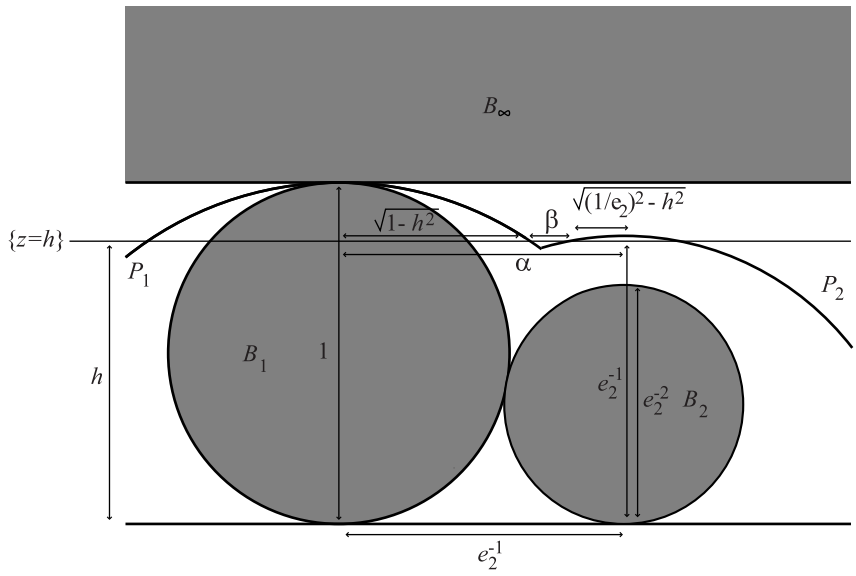

FIGURE 9

When $e_2 > \sqrt{2}$,

$$\frac{\text{Length}(\alpha \cap Q_h)}{\text{Length}(\alpha)} \geq \text{RelLength}(e_2, h).$$

Let P_1 and P_2 be the faces of $\tilde{S}$ containing the endpoints of a lift of α. These are equidistant planes between B_∞ and, respectively, B_1 and B_2.

Let us consider the case where $e_2 > \sqrt{2}$ first, as here the argument is much simpler. Because $e_2 > \sqrt{2}$, $\text{RelLength}(e_2, h)$ is identically zero when $h \leq 1/e_2$. Thus, we may assume that $h > 1/e_2$. The faces P_1 and P_2 contain the endpoints of the lift of α, and therefore they intersect the horosphere $\{z = 1/e_2\}$. The planes equidistant between B_∞ and any horoball other than an $\mathcal{O}(1)$ horoball do not reach as high as $\{z = 1/e_2\}$. Thus, B_1 and B_2 must be $\mathcal{O}(1)$ horoballs. The distance in ∂B_∞ between their orthocenters is therefore at least e_2. Hence, it is clear that the ratio of the lengths of $\alpha \cap Q_h$ and α is at least that of Figure 7, which proves Claim 2 when $e_2 > \sqrt{2}$.

Thus, we now assume that $e_2 \leq \sqrt{2}$. If B_1 and B_2 are both $\mathcal{O}(1)$ horoballs, then, as above, the ratio of the lengths of $\alpha \cap Q_h$ and α is at least that of Figure 6, which proves the claim in this case. Thus, we may assume that at least one of the horoballs (B_2, say) is not an $\mathcal{O}(1)$ horoball. Let us suppose, for the sake of being definite, that the distance between B_1 and B_∞ is no more than that between B_2 and B_∞. We will shortly perform some modifications to B_1 and B_2. We will maintain each plane P_i as the equidistant plane between B_i and B_∞. Thus, P_i will be modified too. Each of these moves will not increase $\text{Length}(\alpha \cap Q_h)/\text{Length}(\alpha)$. So, if we can show that the required lower bound on $\text{Length}(\alpha \cap Q_h)/\text{Length}(\alpha)$ holds after these modifications, then it also held before. In addition, each of these modifications will not decrease the radii of B_1 and B_2. Hence, it will remain the case that the endpoints of α do not lie in Q_h.

Translate B_1 and B_2 towards each other until they become tangent. This reduces the lengths of $\alpha \cap Q_h$ and α by the same amount, and so does not increase the ratio $\text{Length}(\alpha \cap Q_h)/\text{Length}(\alpha)$. We next slide B_1 along B_2, keeping them both just touching and moving the point $B_1 \cap B_2$ closer to B_∞. This has the effect of enlarging B_1 and moving the orthocenter of B_1 away from the orthocenter of B_2. Thus, $\text{Length}(\alpha)$ increases. Also, the union of $B_1 \cup B_2$ and everything below $B_1 \cup B_2$ has increased. Thus, the subset of $P_1 \cup P_2$ consisting of points equidistant from B_∞ and $B_1 \cup B_2$, has moved upwards. In particular, the old $\alpha \cap Q_h$ contains the new $\alpha \cap Q_h$, and therefore the length of $\alpha \cap Q_h$ has not increased. Note that we are using here the fact that the endpoints of α do not lie in Q_h. Stop enlarging B_1 when it becomes tangent to B_∞.

Next perform a similar slide, but with the roles of B_1 and B_2 reversed, until the Euclidean diameter of B_2 is e_2^{-2}. Then, the horoballs are as shown in Figure 9, and so

$$\frac{\text{Length}(\alpha \cap Q_h)}{\text{Length}(\alpha)} \geq \text{RelLength}_2(e_2, h).$$

Thus, we have proved Claim 2.

Claim 1 quickly follows from Claim 2 when $e_2 > \sqrt{2}$, because

$$\begin{aligned}\text{Length}(G \cap Q_h) &\geq \sum_\alpha \text{Length}(\alpha \cap Q_h) \\ &\geq \text{RelLength}(e_2, h) \sum_\alpha \text{Length}(\alpha) \\ &\geq \text{RelLength}(e_2, h) k \text{ Length}(s)/h,\end{aligned}$$

as required. To prove Claim 1 when $e_2 \leq \sqrt{2}$, we must compare $\text{RelLength}(e_2, h)$ and $\text{RelLength}_2(e_2, h)$. Returning to the definitions of these functions, we see that we must compare

$$\frac{2}{e_2}\sqrt{1-h^2} \quad \text{and} \quad e_2\sqrt{1-h^2} + \sqrt{\max\{0, 1-e_2^2h^2\}}.$$

When $1 - e_2^2h^2 \leq 0$, the former is larger because $2/e_2 \geq e_2$. When $1 - e_2^2h^2 > 0$,

$$\begin{aligned}&\frac{2}{e_2}\sqrt{1-h^2} \geq e_2\sqrt{1-h^2} + \sqrt{1-e_2^2h^2} \\ \Leftrightarrow\ &(\frac{2}{e_2} - e_2)\sqrt{1-h^2} \geq \sqrt{1-e_2^2h^2} \\ \Leftrightarrow\ &\left(\frac{4}{e_2^2} - 4 + e_2^2\right)(1-h^2) \geq 1 - e_2^2h^2 \\ \Leftrightarrow\ &\frac{4}{e_2^2} - 5 + e_2^2 - \frac{4h^2}{e_2^2} + 4h^2 \geq 0 \\ \Leftrightarrow\ &4h^2\left(1 - \frac{1}{e_2^2}\right) \geq \left(\frac{4}{e_2^2} - 1\right)(e_2^2 - 1) \\ \Leftrightarrow\ &h^2 \geq \left(1 - \frac{e_2^2}{4}\right).\end{aligned}$$

Thus, when $h^2 \geq 1 - (e_2^2/4)$, $\text{RelLength}_2(e_2, h) \geq \text{RelLength}(e_2, h)$. Moreover, we have equality when $h^2 = 1 - (e_2^2/4)$. But when $h^2 = 1 - (e_2^2/4)$, we see from Figure 6 that $\alpha \cap Q_h$ is a single point and so $\text{RelLength}(e_2, h)$ is zero. Hence, $\text{RelLength}_2(e_2, h)$ is also zero. Since RelLength and RelLength_2 are non-decreasing

functions of h, we deduce that they are both zero when $h^2 < 1 - (e_2^2/4)$. Thus, $\mathrm{RelLength}(e_2, h)$ is, for all values of h, the minimum of the two quantities.

This proves Claim 1 and hence the proposition. □

5. Area control

As discussed in Section 2, if we can get good lower bounds for the area of the cusp torus of $M = \mathbb{H}^3/\Gamma$, then we will be able to fruitfully control the number of possible exceptional slopes. We now begin developing this area control by analyzing the maximal cusp diagram for M.

Consider our standard, normalized lift of the cusp neighborhood to upper-half-space. The view from infinity consists of a collection of overlapping disks. Specifically, we vertically project all horoballs other than B_∞ to the plane $z = 1$, thereby producing a collection of disks, the largest of which have radius one-half. Let σ be a parabolic transformation in Γ that preserves B_∞ and has minimal translation length. We may rotate the picture about the $z-$axis so that σ takes $(0, 0)$ to $(m, 0)$ where $m > 0$. Note that, automatically, $m \geq 1$. We take τ to be another element of Γ, so that σ and τ together generate the stabiliser of B_∞. We can assume that τ takes $(0, 0)$ to (tm, h) where $-1/2 < t \leq 1/2$ and $h > 0$. The *maximal cusp diagram* $\mathcal{M}$ for M consists of this euclidean plane with all the vertically projected disks, and arrows representing σ and τ. Quotienting the maximal cusp diagram by the stabiliser of B_∞ produces the cusp torus.

Each orthoclass $\mathcal{O}(i)$ is an equivalence class of horoballs. The image of these horoballs in $\mathcal{M}$ is a collection of disks. They come in two orbits under the action of the stabiliser of B_∞. (The fact that there are two orbits was first observed by Adams [1]. For a horoball B_i other than B_∞, an associated *Adams* horoball is any horoball in the same orthoclass but that is not a translate of B_i under the action of the stabiliser of B_∞.) Thus, the image of these horoballs in the cusp torus is two disks with disjoint interiors, which we denote D_i and D_i'. We also refer to the disks in $\mathcal{M}$ as $\mathcal{O}(i)$ disks.

The disks D_1 and D_1' each have radius one-half and so they contribute $2\pi(1/2)^2 = \pi/2$ to the area of the cusp torus.

We now want to use the next largest disks D_2 and D_2' in the cusp torus to get more area. We observe that if $o(2)$ is small (that is, close to 0) then the D_2 and D_2' disks are large (radius close to one-half), while if $o(2)$ is large, then the D_2 and D_2' disks are small.

By Lemma 3.2, if an $\mathcal{O}(i)$ disk and an $\mathcal{O}(j)$ disk have associated horoballs separated by $o(k)$ then the distance between their centers is $e_k/(e_i e_j)$. By Lemma 3.1, any two $\mathcal{O}(1)$ disks in $\mathcal{M}$ must have centers separated by at least e_2. Hence, we can extend the D_1 and D_1' disks to have radius $e_2/2$ and still have their interiors be disjoint. So, $2\pi(e_2/2)^2 = \pi e_2^2/2$ is a lower bound for the area of the cusp torus. Let D_1^+ denote the union of these two enlarged disks.

Further, we can add on the area provided by the D_2 and D_2' disks. These disks have radius $1/(2e_2^2)$. But we need to take into account the fact that the D_1^+ and D_2/D_2' disks might overlap. The largest overlap occurs when the associated horoballs are abutting; in which case their centers are a distance $e_1/(e_1 e_2) = 1/e_2$ apart. Another problem is that there may be more than one overlap. For example, a D_2/D_2' disk might be overlapped by both D_1^+ disks.

In order to control the number of overlaps, we use Mom technology (see Section 3). Loosely, the theme is that too much overlap leads to Mom structures. Note that in the case of no overlaps, we have the nice situation that when e_2 is "large" we get a big area contribution from $2\pi(e_2/2)^2$ alone, and in the "small" e_2 situation the D_2 and D_2' disks are big and so we still get a "big" area.

Assuming that M does not contain a geometric Mom-2 involving $\mathcal{O}(1)$ and $\mathcal{O}(2)$, it turns out that we can quickly improve our previous estimate, as follows, provided $e_2 \leq 2$. Simply expand the D_1^+ disks to radius $e_3/2$ (not simply radius $e_2/2$). This will result in overlap if the centers of two $\mathcal{O}(1)$ disks are within e_2 of each other. But the overlap can be controlled because we are in the no-Mom-2 situation. Further, we put disks D_2^+ of radius $e_3/e_2 - e_3/2$ centered at the D_2 and D_2' disks (this radius is chosen so as to give fruitful area, but to avoid overlap not handled by the no-Mom-2 condition). Note that $e_3/e_2 - e_3/2 \geq 0$, since $e_2 \leq 2$. If the two D_1^+ disks intersect or if one of the D_1^+ disks is not embedded, then the two associated horoballs are separated by $o(1)$ or $o(2)$, since if they were separated by $o(n)$ for some $n \geq 3$, then their orthocenters would be at leasy e_3 apart, by Lemma 3.2. So, this sort of overlap leads to a $(1,1,1)$ or $(1,1,2)$ triple. But a $(1,1,1)$ triple is ruled out by Lemma 3.1. On the other hand, if a D_1^+ disk overlaps with a D_2^+ disk, then the distance between their orthocenters is less than $(e_3/2)+(e_3/e_2-e_3/2) = e_3/e_2$, and so by Lemma 3.2, the associated horoballs are $o(1)$ or $o(2)$ separated, leading to a $(1,2,1)$ or $(1,2,2)$ triple. And finally, if a D_2^+ disk is non-embedded or if the two D_2^+ disks overlap, then the associated horoballs are $o(1)$ or $o(2)$ separated. This is because otherwise we obtain the inequality $2(e_3/e_2 - e_3/2) > e_3/e_2^2$, which is impossible. Since a $(2,2,2)$ triple cannot occur, we deduce in this case that there is a $(1,2,2)$ triple. Thus, in summary, we have to consider two types of overlap, arising from a $(1,1,2)$ or $(1,2,2)$ triple. The no-Mom-2 condition means that we have to consider the overlap from just one such triple.

First, the $(1,1,2)$ case where there are three horoballs $B_1,\ B_2,\ B_3$ which form a $(1,1,2)$-triple. In $\mathcal{M}$, this manifests itself as 3 overlaps, one for each of the 3 horoballs being sent to B_∞ by an element of Γ. Thus, because B_1 is $o(1)-$separated from B_2 and B_3, then mapping B_1 to B_∞ results in two $\mathcal{O}(1)$ disks whose centers are a distance e_2 apart. This results in an overlap because the expanded disks have radius $e_3/2$. Sending B_2 to B_∞ results in an $\mathcal{O}(1)$ disk and an $\mathcal{O}(2)$ disk whose centers are separated by $e_1/(e_1e_2) = 1/e_2$ and again there is overlap for the expanded disks at these centers. Sending B_3 to B_∞ produces the same overlap picture.

However, because we are assuming that M does not have a geometric Mom-2 involving $\mathcal{O}(1)$ and $\mathcal{O}(2)$, there are no other overlaps between the D_1^+ and D_2^+ disks. Thus, in the case where there is a $(1,1,2)$-triple, we get the following area lower bound for the cusp torus:

$$2\pi(e_3/2)^2 + 2\pi\left(\frac{e_3}{e_2} - \frac{e_3}{2}\right)^2 - \text{overlap}(e_3/2, e_3/2, e_2) \\ - 2\ \text{overlap}\left(\frac{e_3}{2}, \frac{e_3}{e_2} - \frac{e_3}{2}, \frac{1}{e_2}\right)$$

where $\text{overlap}(a,b,c)$ is the area of the overlap of two disks of radius a and b whose centers are separated by c.

The second case is when there is a $(1,2,2)$-triple and here the lower bound for area is:

$$2\pi(e_3/2)^2 + 2\pi\left(\frac{e_3}{e_2} - \frac{e_3}{2}\right)^2 - 2\ \text{overlap}\left(\frac{e_3}{2}, \frac{e_3}{e_2} - \frac{e_3}{2}, 1\right) - \text{overlap}\left(\frac{e_3}{e_2} - \frac{e_3}{2}, \frac{e_3}{e_2} - \frac{e_3}{2}, \frac{1}{e_2^2}\right)$$

By analyzing the overlap function, it can be seen that to find a valid lower bound only the $(1,1,2)$ case is needed. In particular, we exploit the following result.

Lemma 5.1. *If $a_1 \geq a_2$, $b_1 \geq b_2$ and $a_1 + b_1 - c_1 \geq a_2 + b_2 - c_2$ then*

$$\text{overlap}(a_1, b_1, c_1) \geq \text{overlap}(a_2, b_2, c_2).$$

Proof. $a_1 + b_1 - c_1$ is the *linear dimension of overlap*, that is, it's the length of the intersection of the physical overlap with the line connecting the centers. So, the first pair of circles (the circles of radius a_1 and b_1) have larger radii and a greater linear dimension of overlap than the second pair of circles. Hence, the area of the overlap is larger for the first pair of circles than for the second pair of circles. The point here is that not only is the overlap wider in the first case (linear dimension of overlap is greater) but also, in the perpendicular direction (to the linear dimension of overlap) the boundaries of the overlap are more vertical because the associated circles have larger radii. □

In comparing the $(1,1,2)$ and $(1,2,2)$ cases, there are 3 overlap comparisons. First compare 112 versus 122. That is, compare the two D_1^+ disks whose centers are e_2 apart with a D_1^+ and D_2^+ disk whose centers are $e_2/(e_1e_2) = 1$ apart. An application of Lemma 5.1 shows the overlap contribution is greater for 112. Next compare 121 and 221, and then compare 211 and 212. (Compare the proof of Lemma 5.3 below.) In both cases, the overlap is greater for the first element in the comparison. Hence, the total overlap area is larger in the $(1,1,2)$ case.

Thus, we have the following result.

Theorem 5.2. *Let M be a compact orientable 3-manifold, with boundary a torus, and with interior admitting a complete finite-volume hyperbolic structure. Suppose that M does not contain a geometric Mom-2 involving $\mathcal{O}(1)$ and $\mathcal{O}(2)$. Suppose also that $e_2 \leq 2$. Then, the area of the cusp torus is at least*

$$2\pi(e_3/2)^2 + 2\pi\left(\frac{e_3}{e_2} - \frac{e_3}{2}\right)^2 - \text{overlap}(e_3/2, e_3/2, e_2) - 2\ \text{overlap}\left(\frac{e_3}{2}, \frac{e_3}{e_2} - \frac{e_3}{2}, \frac{1}{e_2}\right).$$

Just using the D_1^+ and D_2^+ disks does not provide enough area for our purposes. So we analyze the $\mathcal{O}(3)$ disks, use e_4, and exploit Mom-3 technology. Assuming $e_2 \leq e_3 \leq 2$, we expand the D_1^+ disks to radius $e_4/2$, we expand the D_2^+ disks to radius $e_4/e_2 - e_4/2$, and we expand the D_3 and D_3' disks to radius $e_4/e_3 - e_4/2$, giving disks D_3^+. To control overlap, we assume that M does not have a torus-friendly geometric Mom-3 involving $\mathcal{O}(1)$, $\mathcal{O}(2)$ and $\mathcal{O}(3)$.

There are a variety of cases where overlaps do not yield a torus-friendly geometric Mom-3 (see Section 5 of [17] for the list) and we need to do overlap analysis for these. We must consider the overlap generated by an (a, b, c) triple, where $a, b, c \in \{1, 2, 3\}$. As in the $(1, 1, 2)$ case, there are (at most) three overlaps, with area

$$\begin{aligned}&\text{overlap}(R(a), R(b), e_c/(e_a e_b)),\\ &\text{overlap}(R(b), R(c), e_a/(e_b e_c)),\\ &\text{overlap}(R(c), R(a), e_b/(e_c e_a)),\end{aligned}$$

where $R(a)$, $R(b)$ and $R(c)$ are the radii of the disks D_a^+, D_b^+ and D_c^+. We now use the following:

Lemma 5.3. *For integers $a, b, c, d, e, f \in \{1, 2, 3\}$ such that $a \geq d$, $b \geq e$ and $c \geq f$,*

$$\text{overlap}(R(a), R(b), e_c/(e_a e_b)) \leq \text{overlap}(R(d), R(e), e_f/(e_d e_e)).$$

Proof. Note first that, in order to prove the lemma, we may assume that two of the inequalities $a \geq d$, $b \geq e$ and $c \geq f$ are actually equalities. Note also that $R(x) = (e_4/e_x) - (e_4/2)$. Hence, $R(a) \leq R(d)$ and $R(b) \leq R(e)$. In order to apply Lemma 5.1, we therefore need to know that

$$R(a) + R(b) - e_c/(e_a e_b) \leq R(d) + R(e) - e_f/(e_d e_e).$$

This is clear if $a = d$ and $b = e$. If $b = e$ and $c = f$, the inequality becomes

$$e_4/e_a - e_4/2 - e_c/(e_a e_b) \leq e_4/e_d - e_4/2 - e_c/(e_d e_b),$$

which is equivalent to

$$\frac{e_4 - (e_c/e_b)}{e_a} \leq \frac{e_4 - (e_c/e_b)}{e_d},$$

and this holds because $e_a \geq e_d$ and $e_4 \geq e_c/e_b$. □

Thus, we see that an (a, b, c)-triple will produce less overlap area than a (d, e, f)-triple if $a \geq d$, $b \geq e$, $c \geq f$. Exploiting this observation, there are two possible cases that result in the maximum total overlap area: $(1, 1, 2), (1, 1, 3)$ and $(1, 2, 3), (1, 2, 3), (1, 1, 2)$. This gives the following result.

Theorem 5.4. *Let M be a compact orientable 3-manifold, with boundary a torus and with interior admitting a complete finite-volume hyperbolic structure. Suppose that M does not contain a torus-friendly geometric Mom-3 involving $\mathcal{O}(1)$, $\mathcal{O}(2)$ and $\mathcal{O}(3)$, or a geometric Mom-2 involving a subset of $\mathcal{O}(1)$, $\mathcal{O}(2)$ and $\mathcal{O}(3)$. Suppose also that $e_3 \leq 2$. Then, the area of the cusp torus is at least the minimum of*

$$\begin{aligned}&2\pi(e_4/2)^2 + 2\pi\left(\frac{e_4}{e_2} - \frac{e_4}{2}\right)^2 + 2\pi\left(\frac{e_4}{e_3} - \frac{e_4}{2}\right)^2\\ &\quad - \text{overlap}(e_4/2, e_4/2, e_2) - \text{overlap}(e_4/2, e_4/2, e_3)\\ &\quad - 2\ \text{overlap}(e_4/2, e_4/e_2 - e_4/2, 1/e_2)\\ &\quad - 2\ \text{overlap}(e_4/2, e_4/e_3 - e_4/2, 1/e_3)\end{aligned}$$

and

$$\begin{aligned}2\pi(e_4/2)^2 + 2\pi\left(\frac{e_4}{e_2} - \frac{e_4}{2}\right)^2 + 2\pi\left(\frac{e_4}{e_3} - \frac{e_4}{2}\right)^2 \\ - 2\ \mathrm{overlap}(e_4/2, e_4/e_2 - e_4/2, e_3/e_2) \\ - 2\ \mathrm{overlap}(e_4/e_2 - e_4/2, e_4/e_3 - e_4/2, 1/(e_2e_3)) \\ - 2\ \mathrm{overlap}(e_4/e_3 - e_4/2, e_4/2, e_2/e_3) \\ - 2\ \mathrm{overlap}(e_4/2, e_4/e_2 - e_4/2, 1/e_2) \\ - \mathrm{overlap}(e_4/2, e_4/2, e_2).\end{aligned}$$

In fact, under certain circumstances, it is possible to improve this yet further. We place disks of radius $1/(e_4e_2) - e_4/e_2 + e_4/2$ at the centers of D_4 and D_4'. It is shown in [17] (in the reasoning preceding Lemma 5.6) that these disks do not overlap with the D_2^+ and D_3^+ disks. Moreover, if $2e_4^2 + 2e_4 - e_2(e_4^2 + e_4 + 1) \geq 0$, then these disks are embedded and disjoint. They might overlap with the D_1^+ disks. However, if $e_2 + 1 \geq e_4^2$, then this triggers a $(1, 1, 4)$-triple. Thus, assuming in addition that M does not have a geometric Mom-2 involving $\mathcal{O}(1)$ and $\mathcal{O}(4)$, there can only be one such overlap. Hence, we obtain the following. (See Lemma 5.6 in [17].)

Theorem 5.5. *Let M be a compact orientable 3-manifold, with boundary a torus, and with interior admitting a complete finite-volume hyperbolic structure. Suppose that M contains neither a torus-friendly geometric Mom-3 involving $\mathcal{O}(1)$, $\mathcal{O}(2)$ and $\mathcal{O}(3)$ nor a geometric Mom-2 involving a subset of $\mathcal{O}(1)$, $\mathcal{O}(2)$, $\mathcal{O}(3)$ and $\mathcal{O}(4)$. Suppose also that $2e_4^2 + 2e_4 - e_2(e_4^2 + e_4 + 1) \geq 0$ and that $e_2 + 1 \geq e_4^2$. Then, the area estimate in Theorem 5.4 can be increased by*

$$2\pi\left(\frac{1}{e_2e_4} - \frac{e_4}{e_2} + \frac{e_4}{2}\right)^2 - 2\ \mathrm{overlap}\left(\frac{e_4}{2}, \frac{1}{e_4e_2} - \frac{e_4}{e_2} + \frac{e_4}{2}, \frac{1}{e_4}\right).$$

Note that when $e_4 < (1 + \sqrt{5})/2$, the condition $2e_4^2 + 2e_4 - e_2(e_4^2 + e_4 + 1) \geq 0$ is satisfied. This is because $e_2 \leq e_4$ and so

$$2e_4^2 + 2e_4 - e_2(e_4^2 + e_4 + 1) \geq -e_4^3 + e_4^2 + e_4 > 0.$$

6. Tools for the parameter space analysis

In this section, we describe our tools for excluding regions of the parameter space. We assume that there is no geometric Mom-2 or Mom-3 as in the hypotheses of Theorems 5.4 and 5.5. Recall from Section 1 that we are using 6 parameters: e_2, e_3, e_4, m, t and h and here, we work as though these parameters are fixed and given. However, in practice, they are only specified to lie within small intervals. The parameters m, t and h specify a lattice, which consists of the orthocenter of an $\mathcal{O}(1)$ horoball and its images under the covering transformations that preserve B_∞. One lattice point is at the origin $(0, 0)$. A closest lattice point to $(0, 0)$ is at $A = (m, 0)$. A closest lattice point with non-zero second co-ordinate lies at $B = (mt, h)$, where $-\frac{1}{2} \leq t \leq \frac{1}{2}$ and $h > 0$. In fact, reflecting the picture if necessary, we may assume that $0 \leq t \leq \frac{1}{2}$.

We warm up by analyzing a few representative parameter points.

First, $e_2 = 2.0,\ m = 2.0,\ h = 3.2$. The fact that $e_2 = 2.0$ tells us that the centers of the full-sized disks in the maximal cusp diagram $\mathcal{M}$ are separated by at least distance 2.0. As above, we can embed 2 disks of radius 1 in $\mathcal{M}$. These contribute area 2π to the area of the cusp torus. By disk-packing, we can improve this lower bound on area to $(2\pi)(2\sqrt{3}/\pi) = 4\sqrt{3}$. Hence, no parameter point with these values for e_2, m, h can be realized because the e_2 value implies that the area of the cusp torus is at least $4\sqrt{3}$ but the values of m and h imply that the area of the cusp torus is 6.4, a contradiction.

Second, $e_2 = 2.0,\ m = 2.0,\ h = 4.0$. There is no immediate area contradiction here, so we analyze slopes in $\mathcal{M}$. By Theorem 4.1, we know the only possible exceptional slopes (p, q) must have associated lattice point $(pm + qtm, qh)$ that is within $L = 6\pi/(\pi + 6 - 3\sqrt{3})$ of the origin. That is, we need to have $(p+qt)^2m^2 + q^2h^2 \leq L^2 \leq 23$, which becomes $(p + qt)^2 \leq (23 - q^2h^2)/(m^2)$. Because $h = 4$ in our example, we can see that there can be no exceptional slopes when $q \geq 2$. When $q = 1$ our equation becomes $(p + qt)^2 \leq (23 - 16)/(m^2) = 1.75$. So, when $q = 1$, we have $|p + qt| \leq 1.33$ and this can occur for at most 3 points. Together with $(1, 0)$, the unique $q = 0$ slope, we end up with at most 4 exceptional slopes for these parameter values. This holds regardless of the values of $e_3,\ e_4,\ t$, and further, it holds when $h > 4$ because then the inequalities work at least as well.

Third, $e_2 = 1.26,\ e_3 = 1.38,\ e_4 = 1.38,\ m = 2.19463$. Ignoring t and h for the time being, we can compute a lower bound for the area of the cusp torus; using Theorems 5.4 and 5.5, we get that the area is at least 4.13103. As above, the formula for possible exceptional slopes (p, q) is $(p+qt)^2m^2 + q^2h^2 \leq L^2$ where L is determined as in Theorem 4.1. Here we will take $h = 4.13103/m$ (if h is less than this number then there is an immediate contradiction).

In particular, when $q = 1$ we have $|p + tq| < 2.50441$. When $t = 0$ this means there are most 5 exceptional slopes with $q = 1$, but when $t = 0.5$ we see that there could be 6 exceptional slopes. For $q = 2$ we get $|p+tq| < 2.01622$. When $t = 0$ this means there are most 2 exceptional slopes with $q = 2$ (note that the (p, q) must be relatively prime pairs of integers), but when $t = 0.5$ we see that there could be 3 exceptional slopes. For $q = 3$ we get $|p + tq| < 0.62201$. When $t = 0$ this means there are no exceptional slopes with $q = 3$, but when $t = 0.5$ we see that there could be 2 exceptional slopes. Adding in the exceptional slope $(1, 0)$ yields a maximum of 8 exceptional slopes when $t = 0$. Further, the analysis holds for larger values of h, so more parameter points are eliminated for free.

But when $t = 0.5$ we have a maximum of 12 exceptional slopes and the associated parameter point is not yet eliminated. So, we do the following simple check: Consider the Adams horoball, and determine how close its orthocenter C is to the vertices of the triangle determined by the origin O, the point $A = (m, 0)$ and the point $B = (tm, h)$. It turns out that there is no point in the triangle which is simultaneously further than 1.26101 from the vertices (1.26101 is the circumradius of the triangle OAB). If this number is less than e_2 then we have an immediate contradiction to the fact that e_2 is the second shortest Euclideanized ortholength. Unfortunately, e_2 is just slightly less than the circumradius, and there is no immediate contradiction. So, we have to do a slightly more complicated check. Because we are assuming that there is no geometric Mom-2 involving $\mathcal{O}(1)$ and $\mathcal{O}(2)$, we see that in actuality, the Adams horoball orthocenter C can be e_2 away from at most

one vertex, and that it is at least e_3 from the other two vertices. By a straightforward calculation, for the parameter point at hand, this can't happen and we have eliminated this parameter point.

In analyzing parameter points we have trivial tools like the one used in the first example above, and we have 3 non-trivial tools: First, compute a lower bound on area and hence an upper bound on the number of exceptional slopes (p, q). Second, use circumradius. Third, bring in the no-Mom-2 assumption to further constrain the possible position of the center of the Adams horoball.

More specifically, Tool 1 is as follows.

Tool 1: For each e_2, e_3 and e_4, compute a lower bound on the area of the cusp torus, using the formulae from Section 5. Then, for each torus with at least this area, use the improved version of the 6-theorem to bound the set of exceptional slopes.

We now describe Tools 2 and 3 in more detail. Tool 2 is used to show that certain regions of the parameter space lead to a contradiction. Tool 3 is used to show that, for certain other regions, M contains a geometric Mom-2 involving $\mathcal{O}(1)$ and $\mathcal{O}(2)$.

Consider the orthocenter C of the Adams horoball. Its distance from each lattice point is at least e_2. In fact, if it closer than e_3 to a lattice point, then this implies that there is a $(1, 1, 2)$-triple of horoballs. So, if it is closer than e_3 to two lattice points, there are two inequivalent $(1, 1, 2)$-triples and so M contains a geometric Mom-2 involving $\mathcal{O}(1)$ and $\mathcal{O}(2)$.

Tool 2: This consists of one test. Check whether there is some point that has distance at least e_2 from all lattice points. If not, this arrangement cannot occur and such parameter points are eliminated. If so, then this arrangement is provisionally permitted. Note that, here, no Mom technology is required.

Tool 3: This consists of two tests:

(1) Check whether there is some point that has distance at least e_3 from all lattice points. If so, then this arrangement is permitted. If not, then pass to the second test.
(2) The orthocenter C is therefore distance less than e_3 from a lattice point, which we may take to be $(0, 0)$. So, it lies within an annulus centered at $(0, 0)$, with inner radius e_2 and outer radius e_3. The second test verifies whether there is a point in this annulus that is distance at least e_3 from every other lattice point. If so, then this arrangement is permitted. If not, then M must contain a geometric Mom-2 involving $\mathcal{O}(1)$ and $\mathcal{O}(2)$.

In order to implement Tool 2 and Test 1 of Tool 3, we compute the circumradius of the triangle T with corners $O = (0, 0)$, $A = (m, 0)$, $B = (mt, h)$, which is

$$\frac{|OA|\ |AB|\ |BO|}{4\mathrm{Area}(T)} = \frac{m\sqrt{m^2(1-t)^2 + h^2}\sqrt{m^2t^2 + h^2}}{2mh}.$$

Clearly, if this is definitely less than e_2, then every point in T has distance less than e_2 from one of O, A and B. Hence, every point in the plane is less than e_2 from some lattice point, and hence this parameter point can be discarded. This is Tool 2. If the circumradius is at least e_3, then Test 1 of Tool 3 passes. Otherwise, we pass to Test 2, which we now describe.

Assuming that Test 1 of Tool 3 has failed, the circumradius of T is less than e_3. Thus, the disks of radius e_3 centered at the corners of T cover T. Hence, the sides of T each have length at most $2e_3$. (Note that the midpoint of each side is closer to

the endpoints of the side than the remaining vertex, because the triangle T is not obtuse.) So, the six primitive lattice points that are closest to O form a hexagon with side lengths less than $2e_3$. Therefore, the disks of radius e_3 centered at these points enclose a region R, as shown in Figure 10. We now define 6 distinguished points. Consider one of the six copies of T with O as a vertex. Place two circles of radius e_3 at its two vertices which are not O. Then we consider the point of intersection between these two circles that is closest to O. This is one of the 6 distinguished points. In Figure 10, these 6 distinguished points are marked with small squares.

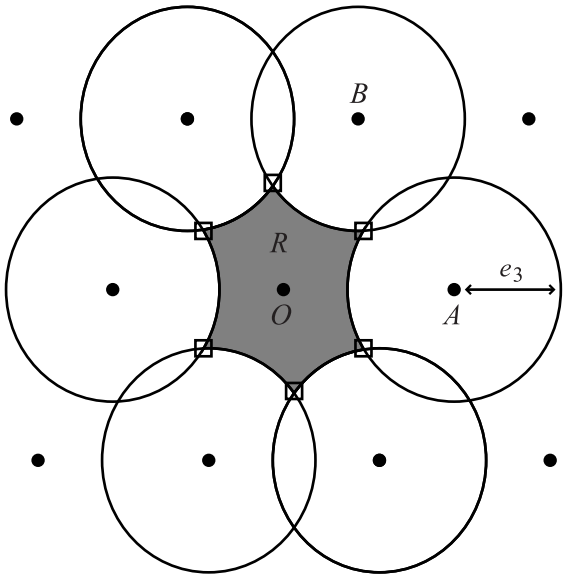

FIGURE 10

Lemma 6.1. *Suppose that Test 1 of Tool 3 has failed. If all 6 of these distinguished points have distance less than e_2 from O, then M contains a geometric Mom-2 involving $\mathcal{O}(1)$ and $\mathcal{O}(2)$.*

Proof. Consider one of the 6 primitive lattice points closest to O. The circle of radius e_3 about this vertex contains two distinguished points. We join these two points by the arc of the circle that is shorter. The union of these arcs forms a closed curve F shaped like a hexagon. The boundary of R forms a subset of F. Typically, the boundary of R will be all of F, but there are situations where it is not. For example, if $|OA| < e_3$, then the disks centered at A and its reflection in the origin overlap.

We claim that a point of F with maximum distance from O is at one of the 6 distinguished points. This follows from the fact that F is a union of arcs of circles. For any such arc, a point of maximal distance from O is at an endpoint of the arc. This is because the unique point of the circle at maximal distance from O is not contained in the arc.

Thus, if all 6 distinguished points have distance less than e_2 from O, then this is true for all points of F, and hence all of R, since ∂R is a subset of F.

Now, if there is no geometric Mom-2 involving $\mathcal{O}(1)$ and $\mathcal{O}(2)$, then C is distance at least e_3 from every lattice point other than O. It therefore misses the interiors of the disks, and so lies in R. But we have seen that every point of R has distance less than e_2 from O, and C is not permitted to lie this close to O. Thus, we deduce in fact that M has a geometric Mom-2 involving $\mathcal{O}(1)$ and $\mathcal{O}(2)$. □

Thus, Test 2 of Tool 3 computes the distances of these six distinguished points from O, and determines whether they are all less than e_2. If so, the configuration is not permitted. Otherwise, it is. In fact, only three of these points need to be tested, since R is symmetric under reflection in the origin and so opposite points have the same distance from O.

7. The parameter space analysis

Here we describe our parameter space analysis in detail. Our first job is to reduce to a compact subset of the parameter space.

We begin by controlling h, m, t.

One crude reduction is to note that when $h > 4$ we can quickly show that no more than 10 exceptional slopes are possible. That is, when $h > 4$, there are no exceptional slopes possible for $q \geq 2$ regardless of the critical slope length $L(e_2)$ from Theorem 4.1, and when $q = 1$ there can be no more that 9 exceptional slopes. Specifically, when $q = 1$, the exceptional slope analysis comes down to $(p + tq)^2 \leq (L(e_2)^2 - h^2)/(m^2) < (36 - 16)/1 = 20$, and we see that $|p + tq|$ must be less than 4.5. Hence, independent of the value of t there can be no more than 9 exceptional slopes when $q = 1$. So, there can be no more than 10 exceptional slopes and the intersection number of any two such slopes is at most 8.

In addition, h must be at least 1.7. For, the fact that m is the minimum translation length implies that $h \geq m\sqrt{3}/2$. Cao and Meyerhoff [9] give that the cusp area is at least 3.35. Thus, $3.35 \leq hm \leq 2h^2/\sqrt{3}$, and hence $h > 1.7$.

Note that this implies that if (p, q) is an exceptional slope, then $|q| \leq 3$. This is because the length of the slope is at least $|q|h$, which is more than 6 when $|q| \geq 4$.

The minimum translation length m must satisfy $m \geq e_2$, by Lemmas 3.1 and 3.2. Further, $m > 2.5$ can be shown to result in at most 8 exceptional slopes. That is, $m > 2.5$ implies that $h > 2$ and hence there are no $|q| \geq 3$ exceptional slopes. For $q = 2$ we get $(p + tq)^2 \leq (L(e_2)^2 - 4h^2)/(m^2) < (36 - 16)/(6.25) < 4$, hence $|p + tq| < 2$ and there are at most 2 exceptional slopes with $q = 2$. Finally, when $q = 1$ we get $(p + tq)^2 \leq (L(e_2)^2 - h^2)/(m^2) < (36 - 4)/(6.25) < 6$, hence $|p + tq| < 2.5$ and there are at most 5 exceptional slopes with $q = 1$. It is also easy to check that in this case, the intersection number of any two exceptional slopes is at most 5. So, we can restrict to $e_2 \leq m \leq 2.5$.

By symmetry, we can assume $0.0 \leq t \leq 0.5$.

Now we control e_2.

When $e_2 \geq 2$, we can use the elementary area argument from Section 6 using disks with radius $e_2/2$ to get good area control. As argued in Section 6, the area of the cusp torus is at least $\sqrt{3}e_2^2$. So if $e_2 \geq 2$, the area of the cusp torus is at least $4\sqrt{3}$. Hence, the intersection number between two slopes with length at most $L(2)$ is no more than $L(2)^2/(4\sqrt{3}) < 3.3$. Hence, using the prime 5 in Agol's bound, we deduce that the number of such slopes is at most 6.

When $e_2 < 2$, we can have the computer analyze the parameter space with m, h, t as restricted above and with $e_2 \leq 2.0$ (the e_3 and e_4 parameters follow, for

free) and show that at each point, the maximum number of exceptional slopes is at most 10 and the intersection number between any two exceptional slopes is at most 8. This is easily done by using interval arithmetic to break up the parameter space into small sub-boxes and then having the computer analyze each small sub-box. The lower area bound of $\sqrt{3}e_2^2$, together with the elementary techniques of Tool 1, establish the theorems as e_2 descends from 2.0 to 1.5. At a little less than $e_2 = 1.5$, the Tool 1 analysis breaks down and we can start applying Tool 2, the circumradius tool. Utilizing this tool enables us to get e_2 down to 1.4. This program is called `slopes1` and is available from the authors [27]. Thus, we can restrict to $1 \leq e_2 \leq 1.4$.

We now work on controlling e_3.

We work under the assumption that $1 \leq e_2 \leq 1.4$. The area control provided by our e_2-only argument is not strong enough in this setting, so we use e_3 as well as e_2 and we exploit Mom-2 technology. In particular, we assume our hyperbolic manifolds contain no geometric Mom-2 involving $\mathcal{O}(1)$ and $\mathcal{O}(2)$, and then use e_2 and e_3 to obtain a lower bound for the area of the maximal cusp torus. To use the Mom approach to area, we need to be able to apply Theorem 3.3 and so we require that $e_2 < 1.5152$. This is certainly the case here. From Theorem 5.2, we get a lower bound for the area of the maximal cusp torus of

$$2\pi(e_3/2)^2 + 2\pi\left(\frac{e_3}{e_2} - \frac{e_3}{2}\right)^2 - \text{overlap}(e_3/2, e_3/2, e_2) \\ - 2\ \text{overlap}\left(\frac{e_3}{2}, \frac{e_3}{e_2} - \frac{e_3}{2}, \frac{1}{e_2}\right).$$

We know that increasing e_3 while holding the other parameters fixed results in an increase in the area bound. The reason is that increasing e_3 while holding the other parameters fixed increases the radii of the relevant disks but does not affect the distance between the centers of the overlapping disks. Now, note that for disks of radius $a,\ b$ with centers c apart, if a is increased then the increase in the overlap is a subset of the annulus which constitutes the increase in the size of the $a-$radius disk. Hence the overall effect is an increase in area even after overlap is accounted for. Now, when using Tool 1 we see that it works better as area increases. Hence, if Tool 1 works for a particular value of e_3 then it works for all larger values because an increase in e_3 here leads to an increase in area (we are assuming, of course, that $1 \leq e_2 \leq 1.4$). In `slopes2`, we fix e_3 to be $51/32$ and use Tool 1 to verify the theorems in this case. Thus, in later routines, we may restrict to $e_2 \leq e_3 \leq 51/32$.

In `slopes3`, we use Tools 1, 2 and 3 to restrict e_3 further: we eliminate parameter points with $1.5 \leq e_3 \leq 51/32$. Thus, in later routines, we may assume that $e_2 \leq e_3 \leq 1.5$. Tool 2 and Tool 3 are a bit trickier here, in that if Tool 2 or 3 works for a particular value of e_3 then it is possible that Tool 2 or 3 does not work for a larger value of e_3. In fact, increasing area makes it easier for Tool 2 and Tool 3 to fail. However, our program is set up so that if Tool 1 fails then the full relevant range of parameter values for m and h are analyzed—in particular, the area of the fundamental parallelograms mh will exceed the (lower bound on the) area given by the above calculation.

We finish up by controlling e_4.

We are now working with $1 \leq e_2 \leq 1.4$ and $e_2 \leq e_3 \leq 1.5$. The above area estimates are inadequate for our methods of eliminating parameter points to work

on these values. We need to utilize e_4 and we now restrict the e_4 parameter values. Thus, we use Theorem 5.4. It follows by roughly the same reasoning as in the e_3 case that if Theorem 5.4 can be used to eliminate a parameter point, then all larger values of e_4 are eliminated too. In fact, the program `slopes4` eliminates points with $e_4 = 51/32$. Thus we can now restrict our parameter space analysis to $e_3 \leq e_4 \leq 51/32$.

We have reduced to the following compact parameter space:
$1 \leq e_2 \leq 1.4$
$e_2 \leq e_3 \leq 1.5$
$e_3 \leq e_4 \leq 51/32$
$e_2 \leq m \leq 2.5$
$1.7 \leq h \leq 4.0$
$0.0 \leq t \leq 0.5$

The rigorous analysis of this parameter space using Tools 1,2, and 3 is straightforward. The relevant program is `slopes5`.

We now discuss computational issues and responses arising from our parameter space analysis. The computer code was written in C++. We use interval arithmetic in the form of `Doubles`. That is, we replace `doubles` by intervals and then develop an arithmetic for these intervals. Specifically, a `Double` x is an interval described by a pair of `doubles` $x = (x.value, x.error)$ where the center of the interval is $x.value$ and the radius of the interval is $x.error$. Following [18], we construct an arithmetic for `Doubles` whereby if two numbers are contained within a couple of `Doubles` x, y then, for example, the `Double` which is the sum of x and y will contain the actual sum of the original two numbers.

In [18] *AffApprox's* are used because of the need for speed. Our needs are considerably less, and we decided to sneak by using `Doubles`. However, because we have 6 parameters, the time constraints were still significant, and we resorted to some tricks to control the time constraints.

The outer loop of the program `slopes5` corresponds to the parameter e_2. Next comes the loop corresponding to e_3, then e_4. At this point, we compute a lower bound for area using Theorems 5.4 and 5.5. The fourth loop corresponds to m, the minimum translation length. Given the `Double` m we can use our area bound to compute a lower bound for h. At this point, we use the functions `CrudeSlopeBound` and `CrudeIntBound` which determine an upper bound for the number of exceptional slopes and an upper bound for the maximal intersection number between exceptional slopes, where both bounds are independent of the parameter t. If we can eliminate a sub-box of parameter points for all values of t by using `CrudeSlopeBound` and `CrudeIntBound`, which is a version of Tool 1, then we have eliminated the associated sub-boxes (same e_2, e_3, e_4, m) with all larger values of h as well. When successful, this is lightning fast, because it is working on a 4-dimensional parameter space.

When `CrudeSlopeBound` and `CrudeIntBound` do not eliminate a sub-box of parameter points then we introduce the parameter t and do a precise count of the possible number of exceptional slopes for parameter points for the sub-box in question by using the functions `FancySlopeBound` and `FancyIntBound`, which are also versions of Tool 1. Again, if we eliminate a sub-box by this approach, then we have also eliminated the associated sub-boxes with larger h as well.

If `FancySlopeBound` and `FancyIntBound` do not eliminate a sub-box, then we want to use Tools 2 and 3. However, these tools don't automatically eliminate larger h values. Thus, we turn h into the sixth parameter and use the 3 Tools to eliminate sub-boxes.

Another technique we used to gain speed was to note that e_4 is only used to get a lower bound on the area of the cusp torus. Hence, when a particular `Double` e_4 produced enough area (in conjunction with the e_2 and the e_3) then if the next e_4 value produced a lower bound for area which was at least as large, then we could simply move on to the next e_4 parameter value without bothering with the Tool analysis. The subtle point here is that because we are only interested in lower bounds here, we compared the low value of the intervals in question.

8. The manifolds in Figure 1

In this section, we explain the method we used to prove the following result.

Theorem 8.1. *Let M be a compact orientable hyperbolic 3-manifold with boundary a torus, and which is obtained by Dehn filling one of the manifolds in Figure 1. Then the number of exceptional slopes on M is at most 7, provided M is not homeomorphic to $m003$, $m004$ or $m009$. Moreover, the intersection number between two exceptional slopes is at most 5, provided M is not homeomorphic to $m003$, $m004$, $m006$ or $m009$.*

To prove this, we could, in principle, apply the following result to each of the manifolds in Figure 1.

Theorem 8.2. *Let N be a compact orientable 3-manifold, the interior of which admits a finite-volume hyperbolic structure. Then there is an algorithm to determine all collections of slopes $(s_0, \dots, s_n)$, with one s_i on each component of ∂N, such that $N(s_0, \dots, s_n)$ is not hyperbolic.*

We will not include a proof of this, since it is a fairly standard application of known algorithms. It relies on the Casson-Manning algorithm [28] for finding a hyperbolic structure on the interior of a compact orientable 3-manifold, if one exists. It also uses normal surface theory algorithms, including a method for computing the JSJ decomposition of a manifold [24] and the 3-sphere recognition algorithm of Rubinstein and Thompson [37]. Thus, it is far from practical.

Instead, we developed a practical procedure which creates a set E of slopes $(s_0, \dots, s_n)$ that contains all the exceptional surgeries. It may be the case that E contains some non-exceptional surgeries, but these are probably rather rare.

So, let N be one of the 3-manifolds in Figure 1. We will deal later with the unique 3-cusped manifold in Figure 1, $s776$. We focus now on the case where N has two boundary components. However, it is clear that this procedure could be extended to deal with manifolds with more boundary components.

The procedure relied on the program Snap [19], which computes hyperbolic structures on 3-manifolds. Its `verify` function uses exact arithmetic based on algebraic numbers. Thus, if the program finds a verified hyperbolic structure, then this is indeed the correct one.

We first used Snap to find the hyperbolic structure on N. We then used Snap to determine a maximal horoball neighbourhood of the cusps, with the property that the neighbourhoods of the two cusps have equal volumes. If s_0 and s_1 are slopes

on distinct boundary components of N that both have length more than 6 with respect to this horoball neighbourhood of the cusps, then by the 6-theorem and the solution to the geometrisation conjecture, $N(s_0, s_1)$ is hyperbolic. Thus, we used Snap to determine all the slopes on the cusp tori with length at most 6.1. (We used 6.1, rather than 6, in order not to worry about slopes with length precisely 6.) For each such slope s_0 or s_1, we needed to determine whether or not $N(s_0, -)$ (or $N(-, s_1)$) has a hyperbolic structure. (Here, $N(s_0, -)$ denotes the manifold obtained by Dehn filling N along the slope s_0, but leaving the second boundary torus unfilled.) If $N(s_0, -)$ is not hyperbolic, then we declare that $\{s_0\} \times S_1$ lies in E, where S_1 is the set of all slopes on the other component of ∂M. (Recall that E is the set of slopes that we are aiming to construct, which contains all the exceptional surgeries.) Similarly, if $N(-, s_1)$ is not hyperbolic, we declare that $S_0 \times \{s_1\}$ lies in E, where S_0 is the set of all slopes on the first boundary torus. The practical method of demonstrating that $N(s_0, -)$ or $N(-, s_1)$ was not hyperbolic was somewhat *ad hoc*, and is described in more detail below.

If $N(s_0, -)$ is hyperbolic, then we used Snap to find this hyperbolic structure and to determine a maximal horoball neighbourhood of its cusp. We then used Snap to find all slopes with length at most 6.1 on this neighbourhood. If s_1 is a slope on this cusp with length more than 6.1, then $N(s_0, s_1)$ is hyperbolic, by the 6-theorem and the solution to the geometrisation conjecture. We then considered the slopes s_1 with length less than 6.1, and used Snap to search for a hyperbolic structure on $N(s_0, s_1)$. If it could not find one, we included (s_0, s_1) in E.

We then performed a similar procedure for the hyperbolic manifolds $N(-, s_1)$, but with the roles of the first and second boundary components swapped.

Occasionally, slightly indirect methods were required to establish that certain slopes were non-exceptional. An example is the surgery $s785((4, 1), (3, 1))$. Snap asserts that this manifold is hyperbolic. But unfortunately, it cannot verify this using exact arithmetic. However, it can show that the manifold $s785(-, (3, 1))$ is isometric to $m222$ and that the isometry preserves Snap's co-ordinate systems for the boundary tori. It can also show that the length of the slope $(4, 1)$ on $m222$ is more than 6.1. Hence, $s785((4, 1), (3, 1))$ admits a hyperbolic structure.

In principle, some surgeries in this set E may not be exceptional. This can happen in two ways. The first situation arises when $N(s_0, -)$ is non-hyperbolic. For example, $N(s_0, -)$ may have non-trivial JSJ decomposition, but $N(s_0, s_1)$ may still be hyperbolic for some s_1. Theorem 8.2 provides a theoretical algorithm for finding all such s_1, but this is not practical. However, the set of such s_1 will probably be rather sparse, and so it did not seem too wasteful to include them in the set E. The second way that E may be too large arose in the search for a hyperbolic structure on $N(s_0, s_1)$, as a Dehn filling of a fixed hyperbolic $N(s_0, -)$. It quite often happens that Snap does not find a hyperbolic structure when one exists. In practice, one may need to use Snap to retriangulate the manifold several times. Even then, manifolds where Snap fails to find a hyperbolic structure may yet have one. Thus, E may be somewhat larger than the actual set of exceptional surgeries. However, it is certainly the case that all exceptional surgeries lie in E. And the procedure was discerning enough to produce Theorem 8.1.

It remains to describe how we dealt with the cases where $N(s_0, -)$ (or $N(-, s_1)$) was not hyperbolic. Here, it is important to prove that $N(s_0, -)$ definitely does not admit a hyperbolic structure, rather than simply declaring that Snap could not

find one. This is because, otherwise, $N(s_0, -)$ might in fact have had a hyperbolic structure, and then be a potential counter-example to Theorem 8.1.

In practice, we proved that $N(s_0, -)$ was not hyperbolic using a variety of methods, all of which utilised a presentation for $\pi_1(N(s_0, -))$. Snap can produce not only this presentation, but also give generators for the peripheral subgroups. We used the following four techniques for proving that $N(s_0, -)$ is not hyperbolic.

(1) If this group presentation is obviously that of a non-trivial free product, then $N(s_0, -)$ is not hyperbolic.
(2) If the existence of a non-trivial center is obvious from this presentation, then again $N(s_0, -)$ is not hyperbolic. In each case, an element of the group was found which commuted with every generator, and which could be seen to be homologically non-trivial.
(3) If the group contains a commuting pair of elements that lie in neither a cyclic subgroup nor a peripheral subgroup, the manifold is not hyperbolic. In practice, both of the required properties of these two elements were verified homologically.
(4) If the presentation has two generators a and b, and the same non-trivial power of a appears in all the relations, the manifold is not hyperbolic. We now supply a proof of this.

Proof. Suppose the presentation is $\langle a, b | w_1(a^k, b), \dots, w_r(a^k, b)\rangle$, where $k > 1$ and the $w_i(a^k, b)$ are words in a^k and b. This group is then an amalgamated free product

$$\langle a\rangle *_{a^k=c} \langle c, b | w_1(c, b), \dots, w_r(c, b)\rangle.$$

Suppose first that this is a trivial amalgamated free product. Then the amalgamating subgroup must be the whole of one of the factors. It cannot be the first factor, since a^k is a proper subgroup of $\langle a\rangle$. Thus, it must be the second factor, which implies that the group is $\langle a\rangle$, which is cyclic. Hence, in this case, the manifold is not hyperbolic. On the other hand, if this is a non-trivial amalgamated free product, then the manifold has non-trivial JSJ decomposition, because the amalgamating subgroup is cyclic. Again, this implies that the manifold is not hyperbolic. □

The following table gives a summary of where these methods were applied. In the first column, the manifold N is given. In the second column, Snap's label for the relevant boundary component is given, which is either 0 or 1. In the third column, the slope s_0 or s_1 is shown, in the co-ordinates given by Snap. The final column gives a number between 1 and 4, according to the method used to prove non-hyperbolicity. It turns out that, in all the manifolds we considered, except $s785$, there exists an isometry of the manifold, swapping the cusps, and preserving Snap's co-ordinate system for the slopes. Thus, in all the cases except $s785$, we only give the slopes on the boundary component labelled 0.

We briefly mention $s780((1, 1), -)$ since this was a slightly tricky case. Snap provides the following presentation of its fundamental group:

$$\langle a, b \mid ab^{-1}a^{-1}ba^2ba^{-1}b^{-1}ab^2\rangle.$$

None of the above four methods can be obviously applied here. However, after re-triangulating, we obtain a new presentation

$$\langle a, b, c \mid bc^{-1}bc^2, aba^{-1}b\rangle.$$

The second relation is that of the Klein bottle fundamental group. Thus, a^2 and b commute. They generate a subgroup of $H_1(M)$ isomorphic to $\mathbb{Z} \oplus \mathbb{Z}/2$, which is

not cyclic. The peripheral subgroup is $\langle bc, ca^{-1}cb^{-1}ca^{-1}c^{-1}\rangle$, which, in $H_1(M)$ is exactly the subgroup generated by a^2 and b. So, this does not immediately lead to a contradiction. However, if a^2 were peripheral, then so would a be. But a does not lie in the image of $H_1(\partial M)$ in $H_1(M)$.

$m412$	0	(1,0)	1	$s785$	0	(1,0)	2
	0	(-1,1)	3		0	(-1,1)	4
	0	(0,1)	2		0	(0,1)	2
	0	(1,1)	3		0	(1,1)	4
$s596$	0	(1,0)	1		1	(1,0)	2
	0	(-1,1)	2		1	(-1,1)	2
	0	(0,1)	2		1	(0,1)	2
	0	(-1,2)	4		1	(1,1)	2
$s647$	0	(1,0)	2	$s898$	0	(1,0)	2
	0	(-1,1)	2		0	(-1,1)	4
	0	(0,1)	2		0	(0,1)	2
	0	(1,1)	4		0	(1,1)	2
$s774$	0	(1,0)	1	$s959$	0	(1,0)	2
	0	(-1,1)	4		0	(-1,1)	2
	0	(0,1)	2		0	(0,1)	2
$s780$	0	(1,0)	2				
	0	(1,1)	3				

We applied the above procedure to the manifolds $m412$, $s596$, $s647$, $s774$, $s780$, $s785$, $s898$ and $s959$. We were able to construct a set E for each manifold N, and thereby verify Theorem 8.1 for any hyperbolic manifold M obtained by Dehn filling N.

As an example, we include here the set E for $m412$. In this case, E is

$$(1,0)\times S_1, \qquad (-1,1)\times S_1, \qquad (0,1)\times S_1, \qquad (1,1)\times S_1,$$
$$S_0\times (1,0), \qquad S_0\times (-1,1), \qquad S_0\times (0,1), \qquad S_0\times (1,1),$$

together with the pairs (s_0, s_1) in the table below marked with an x.

	(-2,1)	(2,1)	(3,1)	(4,1)	(5,1)	(-1,2)	(-1,3)
(-2,1)						x	x
(2,1)		x	x	x	x		
(3,1)		x	x				
(4,1)		x					
(5,1)		x					
(-1,2)	x						
(-1,3)	x						

Here, the slopes along the top are on boundary component 0, and those down the left are on boundary component 1. So, for instance, $M((2,1),-)$ is a hyperbolic manifold with at most 8 exceptional surgeries: $(1,0)$, $(-1,1)$, $(0,1)$, $(1,1)$, $(2,1)$, $(3,1)$, $(4,1)$, $(5,1)$. In fact, $M((2,1),-)$ is $m009$, which is known to have precisely 8 exceptional surgeries.

The sets E for the manifolds $s596$, $s647$, $s774$, $s780$, $s785$, $s898$ and $s959$ can be found in the appendices.

For each manifold with more than 7 exceptional slopes, or where the intersection number between two exceptional slopes is more than 5, we need to prove that it

is one of the manifolds in Theorem 8.1. This is achieved using Snap's `identify` command.

This leaves one remaining manifold from Figure 1, $s776$. This has three boundary components. So, although the above procedure can, in principle, be applied here, it is less practical. Fortunately, Martelli and Petronio [29] have determined all the exceptional surgeries on this manifold M. In particular, Corollary A.6 in [29] implies the first part of Theorem 8.1 in this case. Also, by going through the explicit list of exceptional surgeries in [29], it is possible to verify the second part of Theorem 8.1. □

Note that the manifolds $m003$, $m004$, $m006$ and $m009$ referred to in Theorem 8.1 all satisfy Theorems 1.1 and 1.2. This therefore completes the proof of these theorems. □

It is natural to ask whether one can use the techniques of this paper to prove stronger forms of Gordon's conjectures. For example, it is conjectured that the complement of the figure-eight knot is the unique one-cusped hyperbolic 3-manifold which has 10 exceptional slopes, and it is conjectured that the figure-eight knot complement and the figure-eight knot sister are the only one-cusped hyperbolic 3-manifolds having two exceptional slopes with intersection number 8. According to Theorem 8.1, these conjectures hold when M is a one-cusped hyperbolic 3-manifold that is obtained by Dehn filling one of the manifolds in Figure 1. Thus, to establish these conjectures, we would need to be able to deal with the general situation, when M is not one of these manifolds. In order to use our arguments, the key would be to establish improved lower bounds on the area of the cusp torus. But these would have to be significantly stronger than those given in this paper.

References

[1] C. Adams, *The noncompact hyperbolic 3-manifold of minimal volume.* Proc. Amer. Math. Soc. 100 (1987) 601–606.

[2] I. Agol, *Bounds on exceptional Dehn filling*, Geom. Topol. 4 (2000) 431–449.

[3] I. Agol, *Bounds on exceptional Dehn filling II.* Geom. Topol. 14 (2010) 1921–1940.

[4] S. Bleiler, C. Hodgson, *Spherical space forms and Dehn filling.* Topology 35 (1996) 809–833.

[5] S. Boyer, *Dehn surgery on knots.* Handbook of geometric topology, 165–218, North-Holland, Amsterdam, 2002.

[6] S. Boyer, X. Zhang, *Finite Dehn surgery on knots.* J. Amer. Math. Soc. 9 (1996) 1005–1050

[7] S. Boyer, X. Zhang, *On Culler-Shalen seminorms and Dehn filling,* Ann. of Math. (2) 148 (1998) 737–801.

[8] S. Boyer, X. Zhang, *A proof of the finite filling conjecture,* J. Differential Geom. 59 (2001) 87–176.

[9] C. Cao, R. Meyerhoff, *The orientable cusped hyperbolic 3-manifolds of minimum volume,* Inventiones math. 146 (2001) 451–478.

[10] P. Callahan, M. Hildebrand, J. Weeks, *A census of cusped hyperbolic 3-manifolds*, Mathematics of Computation, Vol. 68, No. 225 (Jan., 1999) 321–332.

[11] M. Culler, C. Gordon, J. Luecke, P. Shalen, *Dehn surgery on knots*, Ann. of Math. (2) 125 (1987) 237–300.

[12] D. Gabai, *Foliations and the topology of 3-manifolds. III.* J. Differential Geom. 26 (1987) 479–536.

[13] D. Gabai, *Quasi-minimal semi-Euclidean laminations in 3-manifolds.* Surveys in differential geometry, Vol. III (Cambridge, MA, 1996), 195–242, Int. Press, Boston, MA, 1998.

[14] D. Gabai, W. Kazez, *Group negative curvature for 3-manifolds with genuine laminations.* Geom. Topol. 2 (1998) 65–77

[15] D. Gabai, R. Meyerhoff, P. Milley, *Volumes of tubes in hyperbolic 3-manifolds.* J. Differential Geom. 57 (2001), no. 1, 23–46.

[16] D. Gabai, R. Meyerhoff, P. Milley, *Mom technology and volumes of hyperbolic 3-manifolds,* Comment. Math. Helv. 86 (2011), no. 1, 145–188.
[17] D. Gabai, R. Meyerhoff, P. Milley, *Minimum volume cusped hyperbolic three-manifolds,* J. Amer. Math. Soc. 22 (2009), no. 4, 1157–1215.
[18] D. Gabai, R. Meyerhoff, N. Thurston, *Homotopy hyperbolic 3-manifolds are hyperbolic.* Ann. of Math. (2) 157 (2003), no. 2, 335–431
[19] O. Goodman, *Snap*, available at www.ms.unimelb.edu.au/∼snap/
[20] C. Gordon, *Dehn filling a survey*, Knot theory (Warsaw, 1995), Polish Acad. Sci., Warsaw 1998, 129–144.
[21] C. Gordon, J. Luecke, *Reducible manifolds and Dehn surgery,* Topology 35 (1996) 385–409.
[22] C. Gordon, Y-Q. Wu, *Toroidal Dehn fillings on hyperbolic 3-manifolds,* Mem. Amer. Math. Soc. 194 (2008), no. 909
[23] C. Hodgson, S. Kerckhoff, *Universal bounds for hyperbolic Dehn surgery.* Ann. of Math. (2) 162 (2005) 367–421.
[24] W. Jaco, J. Tollefson, *Algorithms for the complete decomposition of a closed* 3*-manifold.* Illinois J. Math. 39 (1995) 358–406.
[25] B. Kleiner, J. Lott, *Notes on Perelman's papers.* Geom. Topol. 12 (2008), no. 5, 2587-2855.
[26] M. Lackenby, *Word hyperbolic Dehn surgery*, Invent. math. 140 (2000) 243–282.
[27] M. Lackenby, R. Meyerhoff, *slopes1, slopes2, slopes3, slopes4, slopes5*, available from the authors at www.maths.ox.ac.uk/∼lackenby
[28] J. Manning, *Algorithmic detection and description of hyperbolic structures on closed 3-manifolds with solvable word problem.* Geom. Topol. 6 (2002) 1–25.
[29] B. Martelli, C. Petronio, *Dehn filling of the 'magic'* 3*-manifold*, Comm. Anal. Geom. 14 (2006) 969–1026.
[30] J. Morgan, G. Tian, *Ricci Flow and the Poincare Conjecture.* Clay Mathematics Monographs, 3. Amer. Math. Soc. 2007.
[31] J. Morgan, G. Tian, *Completion of the proof of the Geometrization Conjecture*, arXiv:0809.4040.
[32] L. Mosher, *Laminations and flows transverse to finite depth foliations, Part I: Branched surfaces and dynamics.* Preprint.
[33] S. Novikov, *Topology of foliations,* Trans. Moscow Math. Soc. 14 (1963), 268-305.
[34] G. Perelman, *The entropy formula for the Ricci flow and its geometric applications*, arxiv:math.DG/0211159
[35] G. Perelman, *Ricci flow with surgery on three-manifolds*, arxiv:math.DG/0303109
[36] G. Perelman, *Finite extinction time for the solutions to the Ricci flow on certain three-manifolds*, arxiv:math.DG/0307245
[37] A. Thompson, *Thin position and the recognition problem for* S^3. Math. Res. Lett. 1 (1994) 613–630.
[38] J. Weeks, *SnapPea*, available from the author at www.geometrygames.org.

Appendix A. Surgeries on $s596$

$(1,0)\times S_1$, $(-1,1)\times S_1$, $(0,1)\times S_1$, $(-1,2)\times S_1$,
$S_0\times(1,0)$, $S_0\times(-1,1)$, $S_0\times(0,1)$, $S_0\times(-1,2)$,

	(-2,1)	(1,1)	(-2,3)	(-1,3)
(-2,1)	x		x	
(1,1)		x		x
(-2,3)	x			
(-1,3)		x		

Appendix B. Surgeries on $s647$

$(1,0)\times S_1$, $(-1,1)\times S_1$, $(0,1)\times S_1$, $(1,1)\times S_1$,
$S_0\times(1,0)$, $S_0\times(-1,1)$, $S_0\times(0,1)$, $S_0\times(1,1)$,

	(-7,1)	(-6,1)	(-5,1)	(-4,1)	(-3,1)	(-2,1)	(2,1)	(-1,2)	(1,2)	(-2,3)
(-7,1)						x				
(-6,1)						x				
(-5,1)						x				
(-4,1)						x				
(-3,1)					x	x				
(-2,1)	x	x	x	x	x	x				
(2,1)								x		x
(-1,2)							x		x	
(1,2)								x	x	
(-2,3)							x			

Appendix C. Surgeries on $s774$

$(1,0)\times S_1$, $(-1,1)\times S_1$, $(0,1)\times S_1$,
$S_0\times(1,0)$, $S_0\times(-1,1)$, $S_0\times(0,1)$,

	(-5,1)	(-4,1)	(-3,1)	(-2,1)	(1,1)	(2,1)	(3,1)	(-1,2)	(-1,3)
(-5,1)				x					
(-4,1)				x					
(-3,1)			x	x					
(-2,1)	x	x	x	x					
(1,1)					x			x	x
(2,1)								x	
(3,1)								x	
(-1,2)					x	x	x		
(-1,3)					x				

Appendix D. Surgeries on $s780$

$(1,0) \times S_1$, $(1,1) \times S_1$,
$S_0 \times (1,0)$, $S_0 \times (1,1)$,

	(-7,1)	(-6,1)	(-5,1)	(-4,1)	(-3,1)	(-2,1)	(-1,1)	(0,1)	(2,1)	(3,1)	(4,1)	(5,1)
(-7,1)								x				
(-6,1)								x				
(-5,1)							x	x				
(-4,1)						x	x	x				
(-3,1)					x	x	x	x				
(-2,1)				x	x	x	x	x				
(-1,1)			x	x	x	x	x	x				
(0,1)	x	x	x	x	x	x	x	x				
(2,1)									x	x	x	x
(3,1)									x	x		
(4,1)									x			
(5,1)									x			

Appendix E. Surgeries on $s785$

$(1,0) \times S_1$, $(-1,1) \times S_1$, $(0,1) \times S_1$, $(1,1) \times S_1$,
$S_0 \times (1,0)$, $S_0 \times (-1,1)$, $S_0 \times (0,1)$, $S_0 \times (1,1)$,

	(-2,1)	(2,1)	(3,1)	(-1,2)	(1,2)
(-2,1)		x	x		x
(2,1)		x	x		
(-1,2)				x	
(1,2)	x				
(2,3)	x				

Appendix F. Surgeries on $s898$

$(1,0) \times S_1$, $(-1,1) \times S_1$, $(0,1) \times S_1$, $(1,1) \times S_1$,
$S_0 \times (1,0)$, $S_0 \times (-1,1)$, $S_0 \times (0,1)$, $S_0 \times (1,1)$,

	(-3,1)	(-2,1)	(2,1)	(-1,2)	(1,2)
(-3,1)		x			
(-2,1)	x	x	x		
(2,1)		x	x	x	
(-1,2)			x		
(1,2)					x

Appendix G. Surgeries on $s959$

$(1,0) \times S_1$, $(-1,1) \times S_1$, $(0,1) \times S_1$,
$S_0 \times (1,0)$, $S_0 \times (-1,1)$, $S_0 \times (0,1)$

	(-3,1)	(-2,1)	(1,1)	(-1,2)	(1,2)	(-2,3)
(-3,1)				x		
(-2,1)		x		x		x
(1,1)			x	x	x	
(-1,2)	x	x	x			
(1,2)			x			
(-2,3)		x				

Mathematical Institute, University of Oxford, Oxford, UK

Department of Mathematics, Boston College, Chestnut Hill, MA